

# BROADBAND SEISMOLOGY AND NOISE UNDER THE OCEAN

Spahr C. Webb  
Scripps Institution of Oceanography  
University of California, San Diego, La Jolla

**Abstract.** Most of our understanding of the Earth's interior has been derived from measurements from global seismic networks, although no network has ever been truly "global" because some 71% of the Earth's surface is underwater. The resulting gaps in coverage produce a biased and incomplete image of the Earth. Work has begun toward establishing permanent observatories on the deep seafloor, although the technical difficulties remain severe. Will these stations be useful, and where and how shall they be established? Data from seafloor observatories will be of poorer quality than continental site data because the sea surface is an important and local source of broadband noise. This noise is derived from wind and waves through direct forcing at long periods and by nonlinear coupling to elastic waves at short periods. Our understanding of the generation and propagation of seismic noise and of wind and wave

climatology can be used to predict the temporal and geographical variability of the noise spectrum and to assess likely sites for permanent seafloor observatories. High noise levels near 1 Hz may raise detection limits for short-period, teleseismic arrivals above  $m_b = 7.5$ , limiting the usefulness of many seafloor sites. Noise levels in deep boreholes will be 10 dB quieter than those at the seafloor, but sensors buried short distances below the seafloor may also provide comparable noise levels and fidelity. The retrieval of data from permanent seafloor observatories remains an unsolved problem, but long-term temporary arrays of ocean bottom seismometers are now being used in regional scale experiments using earthquakes as sources. Such experiments are likely to be less successful in the Pacific basin than in either the Indian Ocean or North Atlantic Ocean because of higher noise levels.

---

## 1. INTRODUCTION AND OVERVIEW

Seismology remains one of the most important techniques for studying the Earth's interior. A long standing problem for seismologists has been the uneven distribution of seismic stations around the Earth. It has not yet been possible to establish stations on the ocean floor. Gaps in data coverage [Wyssession, 1996] lead to bias in images of the Earth's interior [e.g., Romanowicz, 1991] and to nonuniform and inaccurate maps of global seismicity. This paper is written during a time when groups in the United States, France, and Japan are working toward instrumenting the ocean floor with permanent, broadband seismometer stations. Seafloor stations appear to be the obvious extension of the current networks, with the eventual goal of a truly global network [Purdy and Dziewonski, 1988]. Many problems must be solved before this becomes a reality. Ocean floor sites are different from continental sites because the ocean surface is an important source of broadband seismic noise, so that high noise levels limit the types of seismic measurements that can be made. This paper reviews what is known about seafloor noise and compares noise measurements with the expected signal amplitudes from earthquakes to estimate detection thresholds for body waves and surface waves.

The recent progress in ocean bottom seismometer (OBS) technology has motivated this paper. Ocean bottom seismometers have been in use since the pioneering work of Ewing and Vine [1938], but until recently the recording capacity and endurance of instruments was grossly inadequate for any type of permanent or semi-permanent installation. The world's OBS fleets are almost exclusively short-period instruments used for microearthquake and seismic refraction studies [e.g., Sauter et al., 1990; Moore et al., 1981]. Large-capacity, low-power, digital recording devices are now readily available, and several experiments with continuous recording of seismic signals over intervals of 8–9 months have been accomplished. The first experiment designed to use teleseismic earthquake signals recorded with an ocean floor array to study the Earth was a tomographic study of Lau basin conducted in 1994 [Zhao et al., 1995].

Permanent seafloor stations will require the development of new technology to retrieve the data. Work has begun toward establishing permanent ocean floor seismic stations in the northwest Pacific basin using an abandoned telephone cable [Butler, 1995] and one seismic station has been established on an abandoned cable between Japan and Guam [Kasahara et al., 1997]. The problem of how to recover data from permanent sea-

floor stations otherwise remains unsolved. A global cellular telephone network based on low-altitude satellites may eventually solve this problem, but retrieval of data from seafloor stations will no doubt remain expensive.

Pressure fluctuation measurements are relatively easy to accomplish on the seafloor, and this paper discusses the relative advantages of pressure measurements compared with measurements from seismometers. Pressure is a measure of volumetric strain. Strain measurements on land are usually difficult to accomplish, and the comparable pressure measurement is seldom made because the signal is so small. For body wave observations, marine pressure records are nearly equivalent to vertical acceleration measurements in utility, and pressure sensors can be used to observe Rayleigh waves.

A question of particular importance to the utility of seafloor seismic stations is how often it will be possible to make measurements of short-period teleseismic arrivals with seismometers installed on the deep seafloor. Seismic noise levels at frequencies near 1 Hz at the ocean seismic network OSN-1 test site [Dziewonski *et al.*, 1992] south of Hawaii were found to be higher than noise levels at any of 75 continental and island stations described in the Peterson [1993] report [Webb *et al.*, 1994]. In 11 recent experiments using ocean bottom seismometers in the Pacific, only one short-period teleseismic arrival was seen. This arrival was from a large earthquake ( $M_s = 7.6$ ,  $m_b = 6.3$ ,  $\Delta = 38^\circ$ ) and was only just perceptible above the noise [Blackman *et al.*, 1995]. Modeling shows that at most Pacific seafloor sites the detection threshold for short-period body waves at distances greater than  $30^\circ$  may exceed  $m_b = 7.5$ . This high detection threshold is a significant problem for all studies that require observations of short-period teleseismic arrivals, including most tomographic studies of the Earth's interior, although installation below the seafloor in boreholes may lower detection thresholds by at least one magnitude unit.

There are several magnitude scales used to describe the size of earthquakes:  $m_b$  describes the amplitude of short-period body waves near 1 Hz,  $M_s$  is derived from the amplitude of 20-s surface waves, and  $M_w$  is related to the earthquake moment. The relationship of these scales to more fundamental measures of earthquake size is complex and problematical (see appendix). The number of earthquakes per unit time falls roughly by a factor of 10 for each unit of magnitude [Scholz, 1990]. Thus earthquakes as large as  $M_s = 6.5$  are relatively common (about 50 per year), and earthquakes larger than  $M_s = 7.5$  occur only a few times per year [Bolt, 1976]. Given the finite lifetime of both experiments and experimenters, high noise levels may render some seafloor sites nearly useless for seismic measurements.

The most energetic components of seafloor noise are the "microseisms" near 7-s period, which also dominate noise at continental sites. The microseism peak is broader in frequency at seafloor sites and is the cause of high seafloor noise levels near 1 Hz. The slope of the

noise spectrum is very steep: at 10 Hz, seafloor noise levels may be lower than levels at even the best continental stations [Walker, 1984]. A small increase in attenuation along the ray path produces a large increase in detection threshold because of the rapidly increasing noise levels with wave period. Low seafloor noise levels above 5 Hz provide a window for the detection of small-magnitude local and regional earthquakes and man-made explosions which may have energy at frequencies extending up to 50 Hz. Arrivals from more distant earthquakes have less energy above 1 Hz, and detection is more difficult. High attenuation under young oceanic crust limits the energy in arrivals from distant earthquakes to frequencies below 0.5 Hz. Arrivals from deep sources sample the attenuative upper mantle only once, have higher frequency, and are more readily detected.

Ocean floor instruments may not significantly improve capabilities for detection and localization of remote (teleseismic) earthquakes in many areas because of high noise levels. The word "teleseismic" can be used to describe any arrival from distances greater than  $10^\circ$ , but in this paper it will refer primarily to arrivals at ranges greater than  $30^\circ$ . It is now possible with continental arrays to detect all earthquakes with  $m_b > 4.5$  almost anywhere in the world [Bolt, 1976]. The greater station density in parts of North America and Europe allows the detection of earthquakes larger than about  $m_b = 3$  in these areas. The detection limit can be much smaller within local networks.

This paper reviews the sparse literature available on the geographic and temporal variability of noise at the seafloor. The role of wind-driven waves in generating short-period noise suggests that the detection limits for short-period arrivals should be much lower at sites where the wind is calm and that the best seismic sites will be found in the low-wind regions within the relatively fixed large-scale patterns of winds over the ocean. Sites with steady, moderate breezes, such as the trades or the westerlies of the Southern Ocean, are likely to always be poor sites for permanent stations. Noise levels are expected to be much lower in the central North Atlantic in summer than in the Pacific, with a correspondingly lower detection threshold. Good short-period records have been made of arrivals from moderate earthquakes during experiments in the North Atlantic and Indian Oceans. Unfortunately, most of the sites proposed for a future global ocean seismic network lie either in the central Pacific or in the Southern Ocean because it is within these basins that there are large regions far from seismic stations. The Southern Ocean is a region of strong winds and therefore high noise levels.

Long-period noise ( $>10$  s) levels at the seafloor are high compared to most continental sites, but comparable to noise levels at the noisier island stations. The role of microseisms, ocean currents, and long-period ocean waves (infragravity waves) is reviewed in determining detection thresholds for long period body waves and

surface waves. Long-period compressional ( $P$ ) and vertically polarized shear ( $SV$ ) waves can be seen in records from the seafloor at teleseismic ranges from earthquakes as small as  $M_s = 5.5$ , but the shapes of these arrivals are distorted by interference between the direct arrival and reverberations within the ocean. The reverberations can make it difficult to determine relative arrival times accurately in regions of rough bathymetry [Blackman *et al.*, 1995]. The apparent arrival time varies with the water depth because depth determines the relative phase of the several reverberations. The effect is much smaller in vertical acceleration records than in pressure records.

Infragravity waves control the ocean floor vertical seismic noise level at periods longer than 30 s. Levels are lower in the North Atlantic than in other oceans because of a quieter ocean wave climate. Noise levels are sufficiently low everywhere to provide good signal to noise ratios (SNRs) for Rayleigh waves to periods as long as 200 s, but it is unlikely that useful normal mode measurements will be obtained from any site on the Pacific seafloor, although these measurements may be possible on the North Atlantic seafloor. Tilt fluctuations due to a variety of causes conspire to make long-period horizontal component measurements very noisy, so that although teleseismic long-period horizontally polarized shear ( $SH$ ) waves are seen from earthquakes larger than about  $M_s = 6.3$ , Love waves have been recorded only from earthquakes at regional ( $<25^\circ$ ) distances in a narrow band below the microseism peak.

The best continental sites are in boreholes, and it is generally assumed that permanent seafloor stations will also be installed in boreholes, but large improvements in signal to noise ratios are expected just through burial to shallow depths. This paper considers the relative advantages of boreholes and shallow burial into sediments. Only modest improvements in short-period signal to noise ratios are expected for vertical seismometers at a depth of 50 m in boreholes compared with sites on the seafloor, with about 10 dB corresponding to a reduction in the detection threshold of about one magnitude unit. Installation to significantly more than 100-m depth provides little additional improvement in short-period records but may be necessary to see any reduction in long-period vertical noise levels.

The paper is in two main sections corresponding to the usual short-period and long-period bands separated by the microseism peak at 0.2 Hz. The short-period band section is subdivided into the very low frequency (VLF) ocean acoustics band above 5 Hz and the microseism band below 5 Hz. The long-period band is subdivided into an "infragravity wave" band below 0.03 Hz and a "noise notch" band between 0.03 and 0.1 Hz.

## 2. TYPICAL NOISE SPECTRA

The ocean surface is the primary seismic noise source for both terrestrial and ocean floor sites. The proximity

of seafloor stations to ocean noise sources and the varying efficiency of seismic noise propagation from the ocean to the continents establishes the different behavior of the noise spectrum at terrestrial and seafloor sites. High-frequency noise propagates poorly from ocean to land, resulting in a quieter noise spectrum near 1 Hz at island stations than at adjacent seafloor sites. Island stations are still noisy in the microseism band [Zhang and Langston, 1995; Li *et al.*, 1994; Peterson, 1993; Hedlin and Orcutt, 1989] compared with most continental sites. Peterson [1993] summarizes noise spectra during quiet intervals from 75 continental and island sites. A comparison of island sites with historical bounds from seafloor noise spectra in the microseism band concluded that short-period noise at seafloor sites could be comparable to noise levels at island sites [Hedlin and Orcutt, 1989], but such quiet conditions are probably rare in the Pacific.

Noise levels vary from site to site on land [Peterson, 1993], as well as between oceans and between sites within an ocean basin. Ocean waves are the most important source of noise within the ocean at seismic frequencies. Obviously, the ocean's surface is considerably more energetic in some areas than in others. Oceanographic signals come from both teleseismic and local sources. The short-period ocean wave field is primarily determined by wind local to the area, whereas long-period waves are produced by large ocean storms and travel thousands of kilometers [e.g., Snodgrass *et al.*, 1966]. The seismic noise generated by the ocean wave field also has local components generated directly overhead and teleseismic components propagating as elastic waves from distant sources.

The general shapes of the deep-sea acceleration and pressure noise spectra in the Pacific have been known since the deployment of a broadband system on a cable offshore of San Francisco in 1965 [Sutton *et al.*, 1965; Sutton and Barstow, 1990]. A typical broadband vertical acceleration power spectrum from the deep seafloor near Hawaii is shown in Figure 1 [Webb *et al.*, 1994]. Shown for comparison are spectra from the nearby island station Kipapa (KIP) and from a typical continental site (Pinyon Flat Observatory, California (PFO)). The spectra look fundamentally similar. The prominent microseism peak at 0.14–0.2 Hz (period of 5–7 s) divides the spectra into long-period and short-period bands. At frequencies between 0.03 Hz and 0.1 Hz and above 5 Hz, the noise at the seafloor in the Pacific is comparable to or lower than that at typical continental sites. The most significant difference between most seafloor sites and continental sites is the very high noise level near 1 Hz. The OSN-1 site is 20–30 dB noisier at 1 Hz than the island site and 40 dB noisier than the quietest land sites [Peterson, 1993].

A band of low noise is usually found at terrestrial sites between the microseism peak at 0.2 Hz and cultural noise sources beginning at about 5 Hz. A similar band of low noise is seen in the ocean floor measurements, but

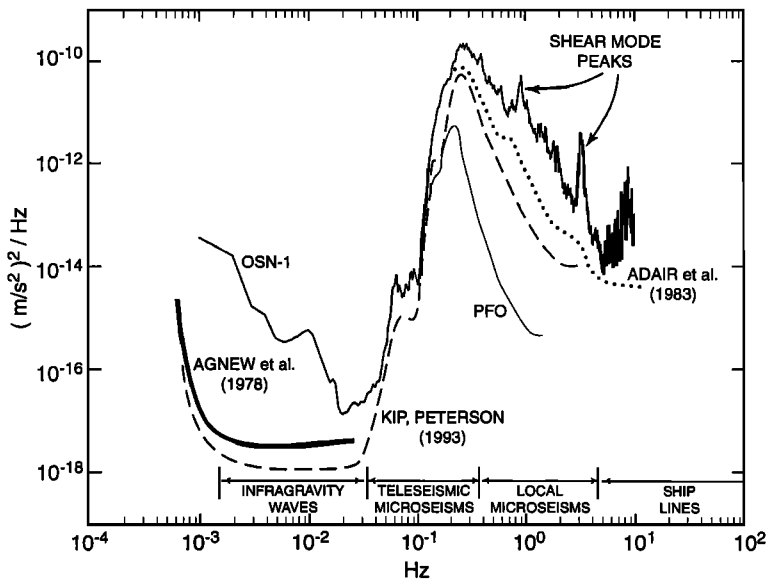


**Figure 1.** Vertical acceleration spectra from the seafloor south of Hawaii (OSN-1); from Kipapa, Hawaii [from *Peterson*, 1993]; and from a quiet site in California (PFO), with the long-period spectrum from the same site [*Agnew and Berger*, 1978]. The microseism peak at 0.2 Hz divides the spectra into long- and short-period bands.

the band is shifted upward in frequency to between 5 and 10 Hz. At 10 Hz the noise level is usually lower than that at even the quietest land sites, which have higher cultural noise [*Walker*, 1984]. Marine refraction and microearthquake studies take advantage of the low noise in this band.

The energy in the vertical acceleration spectrum is high at long periods (>50 s) at OSN-1 and other Pacific sites, but not incomparable to the noisier island sites. The Atlantic and Arctic seafloors are usually quieter than Pacific sites at long periods, perhaps reaching the level of quiet continental sites.

Measurements of pressure variation are relatively simple to make over a broad frequency band and do not involve the problem of coupling inertial sensors to ground motion on very soft seafloor sediments. Pressure measurements can be made either with conventional hydrophones or with differential pressure gauges [*Cox et al.*, 1984]. The differential pressure gauge has lower instrumental noise than the best conventional long-period hydrophones at frequencies below the microseism peak, but it is noisier at frequencies above 1 Hz. A disadvantage of pressure records is that horizontally polarized shear waves and Love waves are absent, unless converted to vertically polarized waves by scattering or anisotropy. Vertically polarized shear waves efficiently couple into compressional waves at the seafloor and are seen with the Rayleigh waves and compressional body waves.

Figure 2 shows examples of pressure spectra from the Pacific, Atlantic, and Arctic seafloors. The microseism peak is again evident between 0.1 and 5 Hz, but the pressure spectrum also rises abruptly at long periods (>0.03 Hz) due to infragravity waves. Noise levels at the seafloor in the North Atlantic tend to be 10–30 dB lower at all frequencies, including the microseism peak, than in the Pacific. The frequency band between the micro-

seisms and the infragravity band has been called the noise notch.

The pressure spectrum varies more with water depth than does the displacement spectrum at long periods because the low acoustic impedance of air leads to nearly perfect reflection of sound incident on the sea

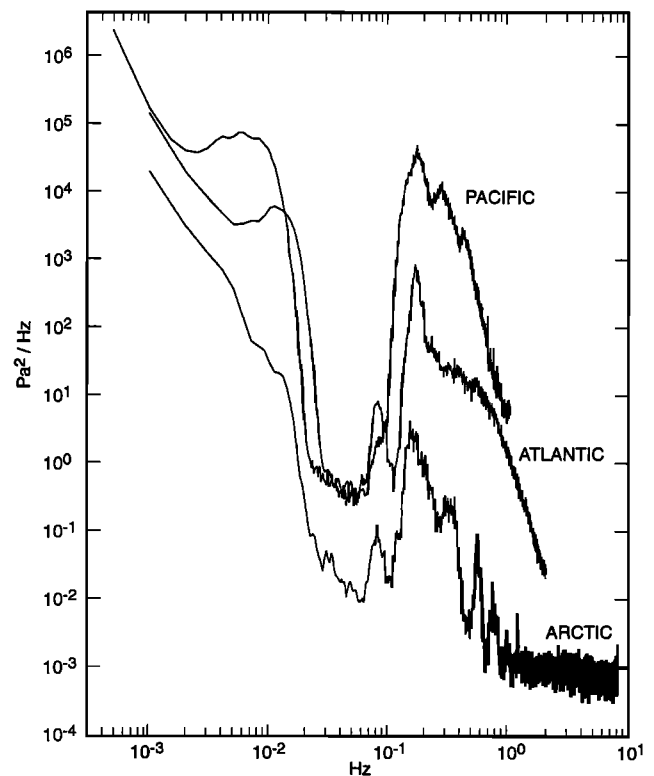


**Figure 2.** Pressure spectra from the seafloor from three oceans. Infragravity waves drive long-period pressure fluctuations below 0.03 Hz. The Arctic and Atlantic are quieter because of a quieter ocean wave climate.

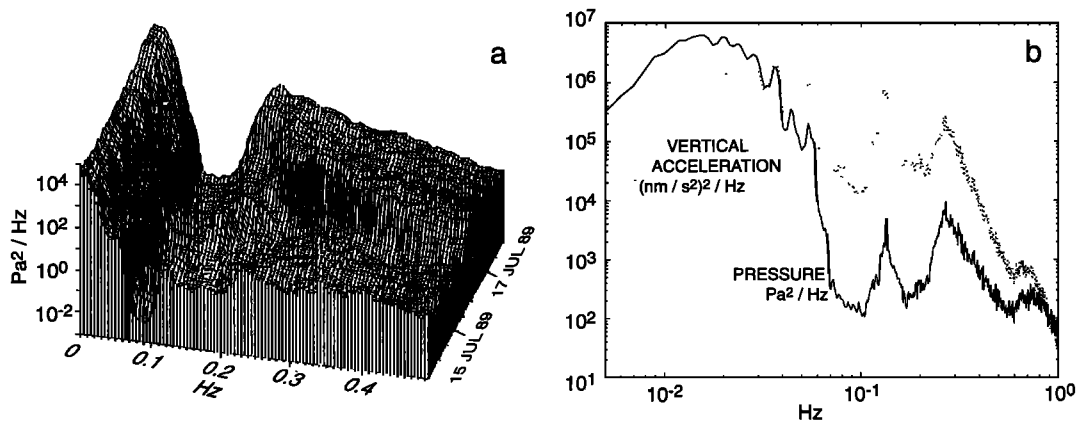


**Figure 3.** (a) A series of pressure spectra from shallow water (600 m) off the coast of southern California. The energy in the microseism peak is very low until late in the record, when a storm directly overhead generates microseisms. (b) Pressure and acceleration spectra from a 1000-m-deep site off the coast of southern California. Energetic infragravity waves drive large vertical accelerations of the seafloor below 0.05 Hz.

surface from below. The reflected wave is of opposite phase in pressure as the incident wave, but of the same phase in vertical displacement. Thus close to the sea surface, the incident and reflected waves add constructively in acceleration but destructively in pressure. Similarly, the pressure signal due to the Rayleigh waves vanishes at the sea surface, while the vertical displacement signal remains finite. The microseism peak in pressure in shallow water looks different from deep water because the teleseismic (Rayleigh) components are attenuated and the peak depends only local excitation by the wave field overhead (Figure 3a). The lower amplitude of the microseism peak in shallow water in pressure does not provide for better detection because the body wave arrivals are similarly reduced by interference with the reflection from the sea surface.

### 3. VLF ACOUSTICS BAND (5–50 HZ)

There is an enormous literature on acoustic noise in the ocean at frequencies above 1 Hz. The noise level between 10 and 50 Hz is mostly controlled by man-made sources, primarily shipping [Wenz, 1962]. Noise in the band from 5 to 10 Hz is associated with wave breaking [McCreery *et al.*, 1993], but large ships can produce energetic spectral lines at frequencies as low as 1 Hz. Whales and other marine mammals also produce significant sound levels above 15 Hz. A spectrogram (Figure 4) shows spectral lines associated with propellers and other rotating machinery, as well as noise from blue and fin whales near 20 Hz. Microearthquakes can be important sources of noise near mid-ocean ridges [McDonald *et al.*, 1995; Riedesel *et al.*, 1982]. At some sites near a ridge axis, a nearly continuous series of microearthquakes can raise the noise level significantly across the entire VLF band [e.g., Sohn *et al.*, 1995]. Richardson *et al.* [1995] provide a recent and detailed discussion of

acoustic noise in the ocean as part of investigation of the effect of man-made noise on marine mammals. Other important reviews of acoustic noise in the ocean are provided by Urick [1983] and Zakarauskus [1986].

The VLF band is the traditional band of marine seismology encompassing signals from microearthquakes and from the air gun and explosive sources used in refraction and reflection studies of the oceanic crust (Orcutt [1987] reviews work in marine seismology). Air gun operations occur almost continuously in the Pacific and the Atlantic and can be a significant source of noise for passive experiments at other sites. Naval sound sources can also control the noise level in the ocean in this band at some times.

The only significant teleseismic phases in the VLF band are the oceanic  $P_n$  and  $S_n$  phases (also called  $P_o$  and  $S_o$  [Walker, 1981]). Attenuation limits the frequencies of teleseismic body waves to less than a few hertz, except for  $P_o$  and  $S_o$ , which travel within the high- $Q$  oceanic lithosphere. These arrivals can have energy at frequencies as high as 15–20 Hz at distances greater than  $30^\circ$  [Walker *et al.*, 1983; Butler *et al.*, 1987]. The long (1–2 min) codas associated with these phases have been ascribed to either scattering by small-scale heterogeneities [Richards and Menke, 1983; Menke and Chen, 1984; Novelo-Casanova and Butler, 1986] or as the result of propagation in leaky organ-pipe modes of the lithospheric waveguide [Serenio and Orcutt, 1985, 1987].

The efficient propagation of  $P_o$  and  $S_o$  phases requires the presence of a low-attenuation oceanic lithosphere. There are many examples where the  $P_o$  and  $S_o$  phases are present on instruments on one side of a ridge crest and not on the other side. On older oceanic crust the efficient propagation of these phases allows the detection of moderate size earthquakes at quite large distances. Walker and McCreery [1985] show several examples of intraplate earthquakes in the western Pacific

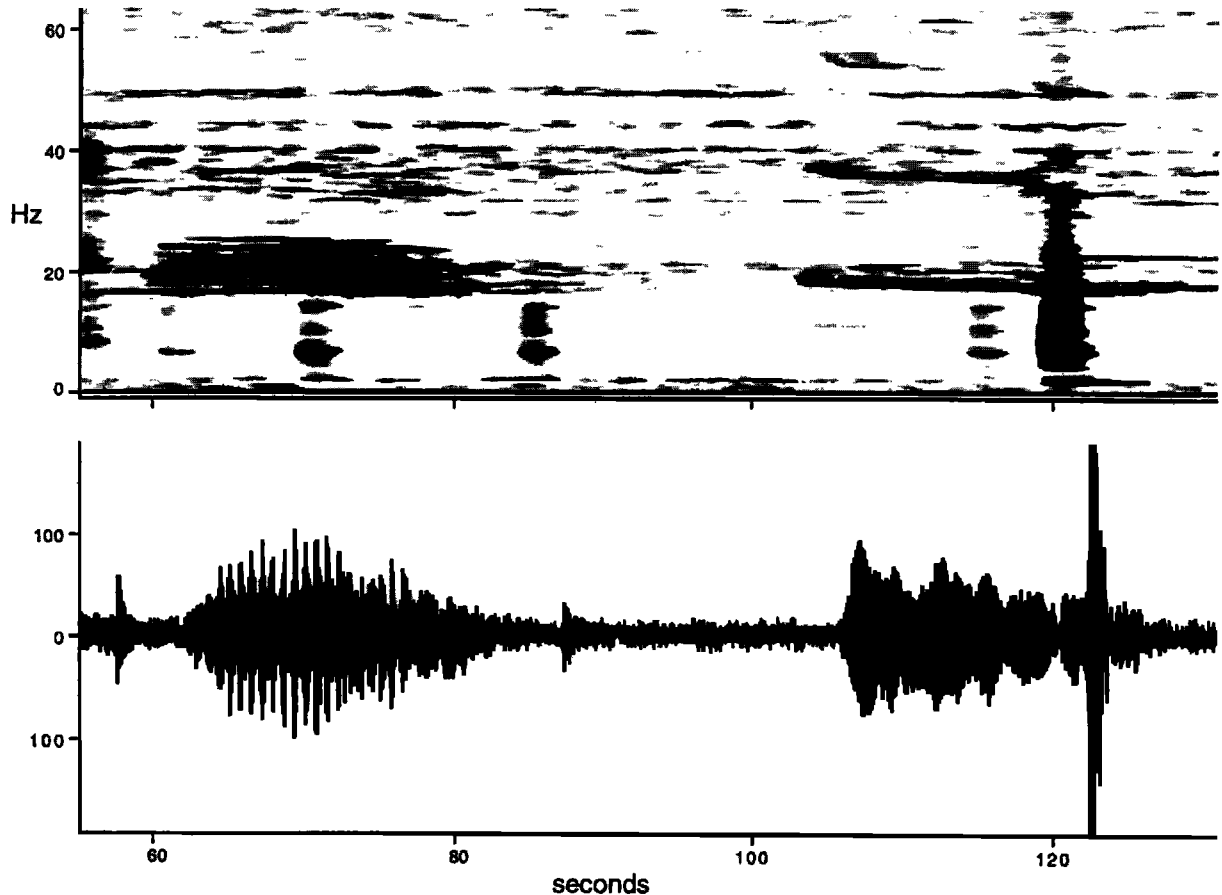


**Figure 4.** (top) Spectrogram showing the spectral intensity as a function of time, and (bottom) the corresponding time record of vertical acceleration. The data are from a site on the Juan de Fuca ridge (reprinted with permission from *McDonald et al.* [1995]; copyright 1995 Acoustical Society of America). Ship machinery produces spectral lines at 20, 40, 50, and 60 Hz. The calls of blue whales appear as 20-s-long signals near 17 Hz. Microearthquakes generate broadband signals near times 70, 85, and 120 s. The spectrogram record is slightly offset (early) from the actual record owing to the finite length of the data windows.

that were recorded on the Wake Island hydrophone array and not at terrestrial sites.

Oceanic earthquakes also couple energy into an acoustic phase traveling in the ocean sound channel called the *T* phase. *T* phases recorded by submarine hydrophones or geophones can be used to determine epicenters for small earthquakes at regional distances. *Fox et al.* [1995] demonstrate an ability to locate earthquakes as small as  $m_b = 2.7$  on the Juan de Fuca ridge using the U.S. Navy SOSUS hydrophone arrays. The array geometry near the Juan de Fuca ridge is well suited for determining earthquake locations. The U.S. Navy acoustic arrays could provide valuable data on earthquake locations in many parts of the ocean and could be particularly useful for locating intraplate earthquakes; however, data from these arrays are not freely available.

#### 4. COUPLING PROBLEM

The typical seafloor installation of an ocean bottom seismometer consists of dropping the instrument into

the water and letting it fall on whatever patch of seafloor is below. This contrasts with the typical land installation, where the instrument is mounted in a vault on a competent piece of ground or is installed into a 100-m-deep borehole. Even a temporary installation often involves digging the instrument into the ground.

Most of the seafloor is covered with a layer of weakly consolidated sediment, with shear velocities as low as 25 m/s [*Schreiner and Dorman*, 1990]. Ideally, a seismometer is installed so that it will track ground motion accurately. In practice, OBSs can be designed with good vertical coupling on soft sediments up to frequencies as high as 25 Hz [*Sutton et al.*, 1981]. The vertical coupling can be modeled as a spring with damping (the soft sediments) and a mass (the seismometer), so that the whole system acts like a simple harmonic oscillator [*Sauter*, 1987; *Duennebieer and Sutton*, 1995; *Sutton et al.*, 1981; *Trehu and Solomon*, 1981]. The sensor package will not respond to ground motion in the sediments at high frequencies, while responding to low-frequency motion. The best broadband frequency response in the vertical is obtained by designing the sensor package to

be approximately neutrally buoyant in water, but horizontal coupling requires some loading of the seafloor. Recent designs have deployed the sensor in a pressure case separate from the recording and recovery hardware, allowing a lightweight package that sits close to the ground. So as to be separated from the larger, heavier recording package, the sensor is dropped from an arm after the instrument lands on the seafloor. The small cross section of the package reduces problems with flow noise. The sensor and recording packages are invariably close enough together that rocking of the recording package in response to arrivals can generate some noise that is reradiated as short wavelength shear modes to the sensor [Trehu and Sutton, 1994].

It is almost impossible to obtain a high coupling frequency for horizontal motion with a sensor deployed on soft sediment. Trehu and Solomon [1981] report a horizontal coupling frequency of 6–10 Hz with a vertical coupling frequency of 22 Hz on soft sediment for the Massachusetts Institute of Technology (MIT) OBS's. For most seismic phases there is differential motion between the water and the seafloor, and the net motion of the sensor is a combination of the seafloor motion and the motion of the water above the seafloor. Horizontal motions of the seafloor must invariably tilt the seafloor sensor package coupling into both horizontal and vertical motions [Duennebier and Sutton, 1995] unless the sensors are installed below the seabed.

In practice, the fidelity of sensor measurements at high frequency has been of secondary importance. The primary interest has been to detect the shear and compressional wave arrivals clearly. The instrument response can be either underdamped or overdamped depending on the design of the sensor package and the properties of the sediment. Underdamped systems "ring," making it difficult to distinguish arrivals following the *P* wave. An experiment studying the response of different OBSs found a wide range of behavior [Zelikovitz and Prothero, 1981]. A tall, heavy instrument can act like an inverted pendulum and ring for many seconds at periods near 1 Hz. Ringing is reduced by designing a sensor package that is low to the ground.

The behavior of OBSs on the rock of the ridge crest is usually better than on sediments. It is possible to see *P* waves from microearthquakes with frequencies as high as 35 Hz, and shear waves at frequencies as high as 15 Hz (Figure 5) on both horizontal and vertical sensors. Studies of the horizontal motion from controlled sources show that the horizontal sensors seldom follow cosine response curves with azimuth for short-period arrivals, so that the two horizontal components are coupled together and to the vertical component [Lewis and Tuthill, 1981]. Nearly the same polarization of particle motions may be observed at a seafloor sensor for refracted arrivals from orthogonal directions [e.g., Bratt and Solomon, 1984; Trehu, 1984], although the horizontal particle motions for waterborne signals may appear consistent. It is not usually possible to use short-period, three-compo-

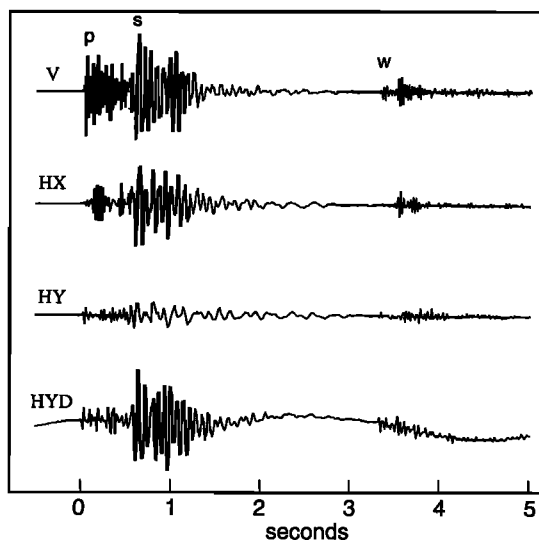


Figure 5. Microearthquake record from a ridge crest. On rock, ocean bottom seismometers can produce records with good fidelity. This record shows the *P* wave at nearly 35 Hz, followed by a 15-Hz shear wave 0.3 s later and by the waterborne arrival. The hydrophone (HYD) provides similar fidelity; the low-frequency oscillation is due to the 6-s microseisms.

nent measurements to infer the azimuth to a microearthquake. Estimates of azimuth from long-period body waves are more consistent, with measured variances of 5°–15° from the expected arrival azimuth (W. Hammond, personal communication, 1987).

The best solution to the coupling problem on sediment is to install the sensor package below the seafloor into the sediment. This can be done either by jetting the sensor into the bottom with a flow of water [Yamamoto et al., 1989], installing it in a caisson [Duennebier et al., 1991], or driving it with a hydraulically driven screw (D. Bibee, personal communication, 1996). Others have suggested pushing the sensor through the sediment under a large weight in a similar manner to a gravity corer. Placing the horizontal sensors below the seafloor interface should greatly improve the fidelity by removing the sensors from the differential motion found at the seafloor. The increasing shear strength at depth will also improve coupling. Another solution to the coupling problem is to install the sensors into boreholes, but it can be difficult to couple the sensor to the uneven wall of the borehole, and the casing of the borehole may not be tightly fixed to the surrounding rock. At periods longer than 1 s, coupling seldom appears to be a problem on either sediments or rock [Duennebier and Sutton, 1995].

## 5. MICROSEISM BAND: (0.1–5 HZ)

The ground motions associated with the spectral peak at 0.2 Hz are called microseisms (Figure 1). Microseisms are caused by ocean waves and propagate mostly as fundamental mode Rayleigh waves. The large peak at

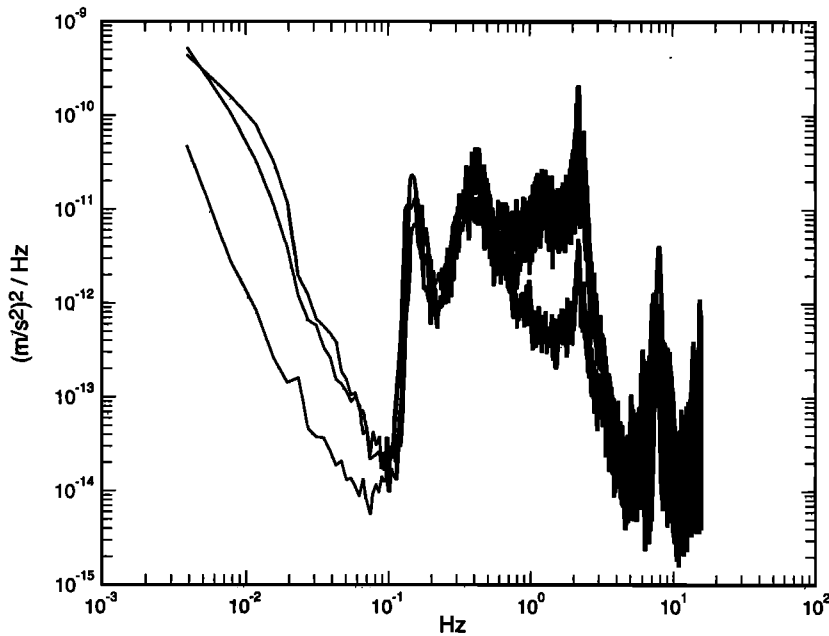


**Figure 6.** Horizontal and vertical component acceleration noise spectra from a 1-Hz seismometer deployed on the East Pacific Rise. Long-period vertical component noise level is determined by instrument noise. Horizontal noise is due to tilt and is quite variable over time. Large shear mode resonances or coupling resonances are very apparent at this site above 3 Hz. These same peaks are not as apparent when presented as a displacement spectrum (Figure 12).

0.2 Hz is called the double-frequency peak. A second, much smaller peak between 0.05 and 0.1 Hz is called the primary or single-frequency peak (discussed later in section 16). The two peaks are created by separate mechanisms.

The microseism peaks are evident in spectra from any site, even far from the coast. Typical vertical acceleration spectra from the Pacific seafloor near Hawaii, from the station Kipapa on Hawaii, and from the Pinyon flat Observatory in California show almost identical spectral amplitudes in the band from 0.05 to 0.2 Hz (Figure 1). The close similarity of these spectra is a consequence of the efficient propagation of Rayleigh waves at periods longer than a few seconds.

Microseism amplitudes on horizontal components are comparable to the vertical component near 0.2 Hz and usually slightly higher at frequencies near 1 Hz (Figure 6). A series of peaks is usually seen in the horizontal component spectra above 1 Hz. These peaks are probably due to short-wavelength shear modes (Stoneley or Scholte waves), but instrument coupling resonances may also contribute.

Vertical noise spectra from islands are usually quieter than ocean floor spectra at frequencies above 0.3 Hz, primarily because the short-period microseisms do not propagate efficiently from deep water onto land. Energetic microseisms driven by local ocean waves are present in ocean floor spectra at frequencies as high as 5 Hz. Usually, three peaks are evident between 0.1 and 1 Hz in spectra from sites the Pacific. The lowest-frequency peak near 0.1 Hz often appears only as a shoulder to the main peak at 0.2 Hz. The lowest-frequency microseisms are excited by the huge waves under the largest storms in the Southern Ocean. The main peak between 0.13 and 0.2 Hz is more variable and is associated with more local storms in the North Pacific. A third

peak at higher frequencies is usually related to the local wind wave field [Webb, 1992].

The microseism noise level near 1 Hz determines whether short-period compressional body waves can be seen from a teleseismic earthquake. The next section discusses the detection limits for short-period body waves at noisy sites like the OSN-1 site. Succeeding sections discuss the source of microseisms and the temporal and geographic variation of short-period noise in the ocean.

## 6. DETECTION LIMITS FOR TELESEISMIC SHORT-PERIOD BODY WAVES AND THE MICROSEISM BAND (0.1–5 HZ)

The acceleration amplitude spectrum of a teleseismic, compressional body wave arrival from a large earthquake is peaked toward frequencies near 1 Hz (Figure 7a; see appendix). The dominant frequency of an arrival depends primarily on the attenuation along the ray path between the earthquake and the receiver. The amplitude of an arrival depends on the size of the earthquake, on attenuation and on source parameters. Figure 7a shows the expected rms amplitude of a compressional wave arrival in one-third octave bands for an earthquake at a distance of 30°. The rms noise levels in the same one-third octave bands from two sites are plotted for reference. One noise spectrum is from a quiet interval from a site on the northern East Pacific Rise, and the other spectrum is from the OSN-1 site near Hawaii [Webb *et al.*, 1994]. The noisier spectrum is more typical of Pacific seafloor sites.

It is expected that an arrival will be detected only if the predicted amplitude substantially exceeds the noise level over some band, *Aki* [1976] shows that the peak *P*

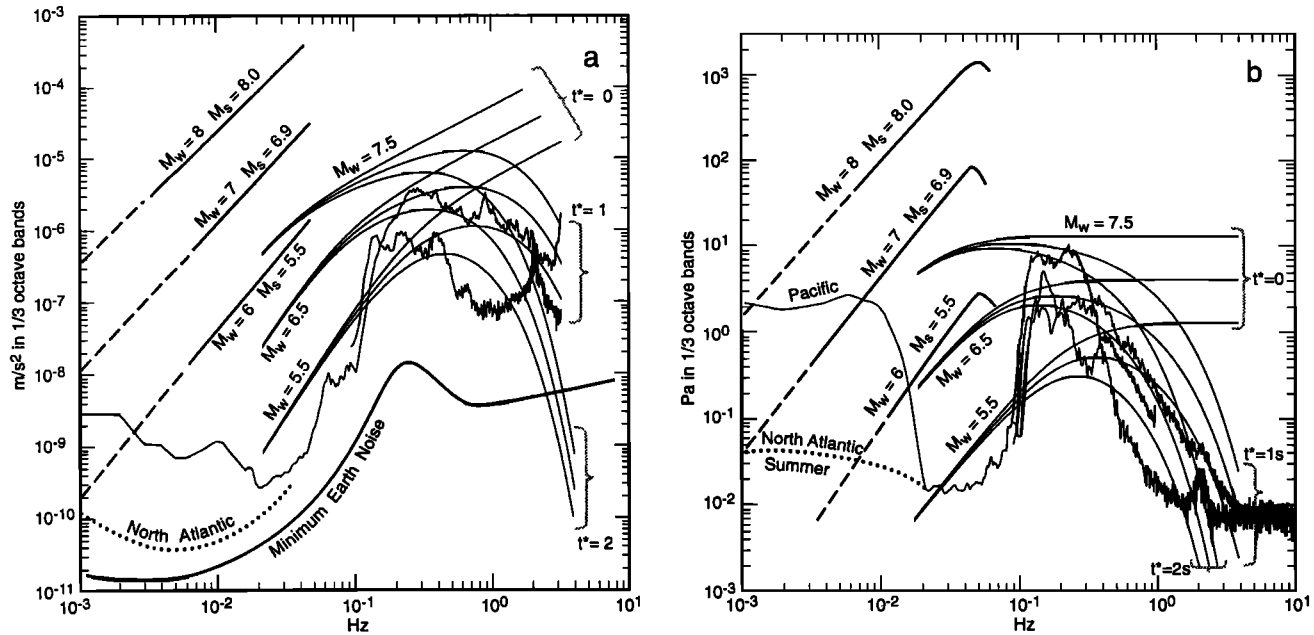


**Figure 7.** (a) Models of the amplitude in the vertical acceleration in one-third octave bands of the  $P$  wave, and surface waves from earthquakes of different magnitudes.  $P$  wave models are plotted for three values of the attenuation parameter  $t$ . The dotted line shows the surface wave models at long periods representing Earth normal mode amplitudes [from *Agnew et al.*, 1986]. Also shown are a quiet and a noisy example of vertical acceleration noise spectra from a site on the East Pacific Rise. It should be possible to detect arrivals in any band for which the signal exceeds the noise significantly. Dashed lines show estimates of the long-period pressure spectrum in the North Atlantic. (b) Same as Figure 7a, but for pressure measurements. Three noise spectra are shown.

wave amplitude must be about 20 times larger than the rms noise to accurately determine an arrival time and the direction of first motion. The useful detection threshold may be lower than this because cross correlation (or simple comparison) of arrivals from one site with another greatly reduces picking error in poor signal to noise situations. This paper assumes that detection will occur when the signal model curves exceed the noise curves by a factor of 6 (16 dB). The 16-dB criterion is used to determine detection thresholds discussed throughout this paper and is consistent with the factor of 20 suggested by Aki if the peak amplitude is assumed to be about 3 times the rms value of the  $P$  wave.

The noise level at the ocean floor falls rapidly with increasing frequency from the peak at 0.2 Hz to the minimum at 5 Hz. Short-period amplitudes increase only slowly with magnitude for large earthquakes, so the detection limit for  $P$  wave arrivals depends strongly on the attenuation along a ray path, which removes the high-frequency components for which the noise background is lower. The frequency dependence of attenuation along a ray path in a medium with frequency independent  $Q$  is described by  $\exp(-t^*f\pi/2)$  (see appendix). Figure 7a shows the amplitude spectrum for three models with  $t^*$  ranging from 0 (no attenuation) to 2 s. At regional distances ( $<10^\circ$ ), body waves from small-magnitude ( $M_b < 3$ ) earthquakes are readily detected between 5 and 10 Hz because attenuation ( $t^* \approx 0$ )

and geometrical spreading are small at these short distances. Regional earthquakes within an ocean basin also produce high-frequency  $P_0$  and  $S_0$  phases that can be seen at large distances.

The preliminary reference Earth model (PREM) predicts  $0.6 < t^* < 1.1$  s for teleseismic  $P$  waves from deep events and  $0.9 < t^* < 1.3$  s for shallow events, with the lower value corresponding to a range of  $25^\circ$  and the upper value to a range of  $95^\circ$  (Figure 8) [Dziewonski and Anderson, 1981]. The value of  $t^*$  is smaller for deep sources than for shallow events because rays travel only once through the attenuative upper mantle. Variations in  $t^*$  with frequency are ignored in the modeling, although measurements show that a significantly smaller  $t^*$  is needed to fit observations near 5 Hz than at 1 Hz [Der et al., 1982] and that a slightly higher  $t^*$  is needed at lower frequencies [Choy and Cormier, 1986]. Regional variation in  $t^*$  contributes to the variability of short period magnitudes with attenuation higher in tectonically active regions than in shield areas. Attenuation in oceanic regions is higher than in continental regions and probably much higher under oceanic ridges, particularly the fast spreading East Pacific Rise [e.g., Ding and Grand, 1993]. The detection limit will be lower on older oceanic crust because the high- $Q$  lithosphere is thicker.

For realistic values of the attenuation parameter for shallow teleseismic earthquakes ( $t^* > 1$ ), the detection limit for short-period body waves will exceed  $m_b = 7.5$

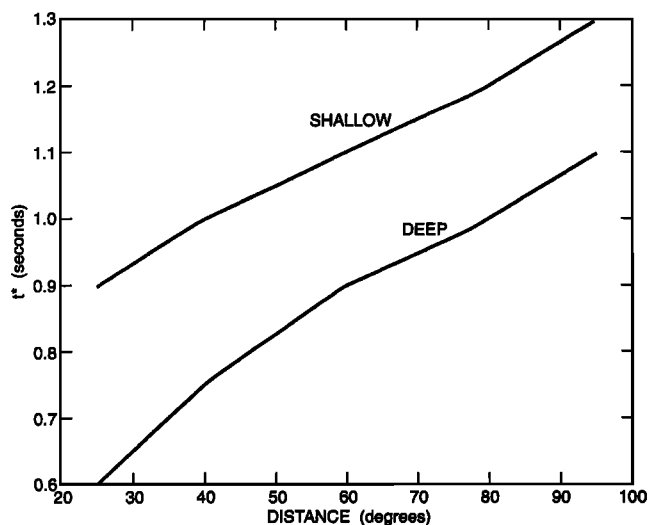


**Figure 8.** The attenuation parameter for  $P$  waves from deep and shallow sources as a function of distance in the preliminary reference Earth model (PREM).

at noisy seafloor sites like OSN-1 (Figure 7a). For small values of the attenuation parameter (associated with deep earthquakes;  $t^* = 0.7$  s) the detection limit falls to  $6.9 m_b$  (Figure 7a). The detection threshold corresponding to the low-noise curve (quiet ocean surface) falls to about  $m_b = 5.5$  for  $t^* = 1$  s and to  $m_b = 5.0$  for  $t^* = 0.7$  s.

A study of records from 11 OBS experiments (mostly at ridge crests) confirms the mostly pessimistic assessment of detection limits from the models presented here, at least in the Pacific basin [Blackman *et al.*, 1995]. Short-period  $P$  waves were seen only in records from the very largest events and at distances less than  $40^\circ$  during these experiments. The short-period  $P$  wave amplitude from a large 1991 Costa Rican event ( $M_s = 7.6$ ;  $\Delta = 38^\circ$ ) exceeded the short-period microseism noise level at the seafloor by only a factor of 2. The  $M_w = 8.3$  Bolivian event of 1994 (the largest in several decades) was well recorded by seismometers on the seafloor near the Juan de Fuca ridge ( $\Delta = 82^\circ$ ) (Figure 9a). The good signal to noise in these records is mostly a consequence of the deep source (636 km [Silver *et al.*, 1995]) with low attenuation along the ray path. The apparent frequency of the  $P$  wave arrival was about 2 Hz. Signal to noise exceeds 25 dB for data low-pass filtered below 6 Hz and exceeds 20 dB for data filtered below 1 Hz. The noise spectrum immediately preceding the event was close to the noisier of the spectra shown in Figure 7a.

In contrast, short-period arrivals have been well recorded during OBS experiments in the Atlantic and Indian Oceans. Rowlett and Forsyth [1979] and Forsyth [1982, 1996], using instruments on the Atlantic seafloor, detected arrivals from four earthquakes with magnitudes from  $m_b = 5.7$  to  $m_b = 6.1$  at ranges from  $39^\circ$  to  $145^\circ$ . Sato *et al.* [1996], using OBSs in the central Indian Ocean, detected short-period arrivals from six earth-

quakes with magnitudes ranging from  $m_b = 5.8$  to  $m_b = 7.2$  with distances between  $72^\circ$  and  $82^\circ$ . The low detection threshold of these two Atlantic and Indian Ocean sites is a consequence of low microseism noise levels at these sites during the experiments. Why these sites are so quiet compared with sites in the Pacific is discussed in section 8.

Horizontal noise levels near 1 Hz tend to be about 10 dB higher than vertical noise levels (Figure 6; see also Figure 15), so that teleseismic, short-period  $P$  waves will be seen only at the quietest sites. Shear waves are usually about a factor of 3 larger and should be seen on the horizontal components whenever the  $P$  wave is visible on the vertical component. Pressure measurements (Figure 7b) are omnidirectional and therefore see higher noise levels than vertical component seismometers. The detection threshold for  $P$  waves is  $\sim 0.2$  magnitude units higher for pressure records.

## 7. MICROSEISM PEAK GENERATION

The high seismic noise level at the seafloor near 1 Hz is caused by the interaction of ocean waves at the surface of the ocean. Longuet-Higgins [1950] first showed how pairs of ocean waves traveling in opposite directions could interact to couple energy into elastic waves. The

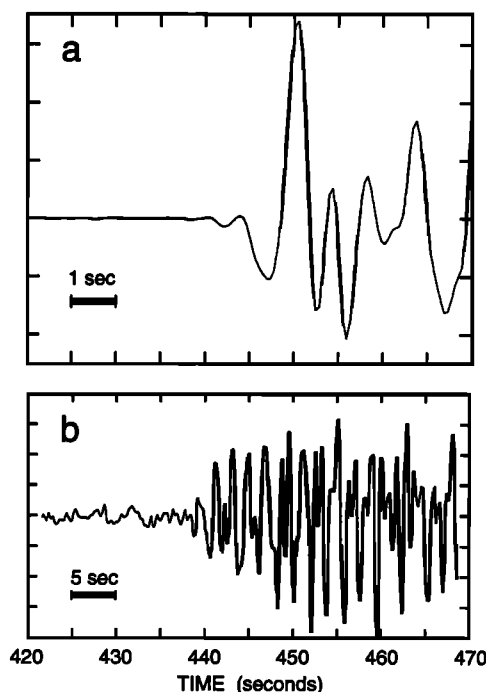


**Figure 9.** The only two examples of short-period  $P$  waves recorded by ocean bottom seismometers (OBSs) in the Pacific. (top) Vertical acceleration record from the 1994 Bolivian earthquake ( $M_s = 8.3$ ,  $\Delta = 82^\circ$ ) recorded on the Juan de Fuca ridge. (bottom) Record from the 1991 Costa Rica event ( $m_b = 6.3$ ,  $M_s = 7.6$ ,  $\Delta = 38^\circ$ ) recorded at  $17^\circ$ S on the East Pacific Rise [from Blackman *et al.*, 1995].

signal from short-period ocean waves otherwise decays rapidly from the sea surface and is not seen at the seafloor. Early work focused on the generation of microseisms at coastlines, where incoming swell could interact directly with the small fraction of ocean wave energy reflected back seaward from the coastline [e.g., *Haubrich et al.*, 1963], but storms at sea were also known to be sources of microseisms [e.g., *Haubrich and McCamy*, 1969; *Cessaro*, 1994]. More recent work has shown a more distributed source for microseisms.

The microseism mechanism has been studied by many researchers; a recent review of the source mechanism is provided by *Kibblewhite and Wu* [1991]. The two fundamental results of the various studies are as follows: (1) the excitation depends on ocean waves traveling in opposing directions, and (2) the frequency is doubled from the ocean wave spectrum into the microseism excitation spectrum. An ocean wave spectrum peaked at 14-s period will generate microseisms at 7-s period. The microseism generation mechanism is more formally described as the result of a triad interaction between two ocean waves of similar frequency and a high-phase velocity wave (acoustic wave) at twice the frequency. The interaction occurs because the ocean surface wave equations are nonlinear at second order. The excitation can be calculated from the frequency and directional spectrum of the ocean wave field [*Hasselmann*, 1963; *Kibblewhite and Ewans*, 1985; *Webb*, 1992].

The ocean wave field consists of wind waves and swell. The term “swell” describes waves from distant sources, and of lower frequency than the local wind-driven waves. Swell is not expected to excite microseisms except near coastlines, where there may be a reflected component to interact with the incident waves. Most microseism energy originates in the deep ocean because the directional spectrum of any wind-driven wave field always includes some energy propagating in opposing directions that can interact to excite microseisms. At any given time, most of the ocean surface is a source of energy in the microseism band. Microseisms at a particular frequency are directly related to ocean waves at half the frequency, so that peaks in the microseism spectrum are observed to evolve in concert with the local wind wave spectrum [*Kibblewhite and Wu*, 1991; *Adair et al.*, 1984; *Webb and Cox*, 1986]. Figure 10 shows an example of an evolving microseism spectrum in the North Atlantic from nearly quiescent conditions during a strong winter storm [from *Babcock et al.*, 1994].

In the Pacific, the microseism spectrum usually has several peaks, only one of which will be related to the local wind wave field. The very lowest frequency (0.1–0.16 Hz) microseisms are generated by largest waves, so these signals are usually “teleseismic,” originating under a few very large storms. The sharp “cliff” on the low-frequency side of the microseism peak at 0.1 Hz is a consequence of the rarity of energetic ocean waves with periods longer than 20 s.

There are several models that describe the evolution

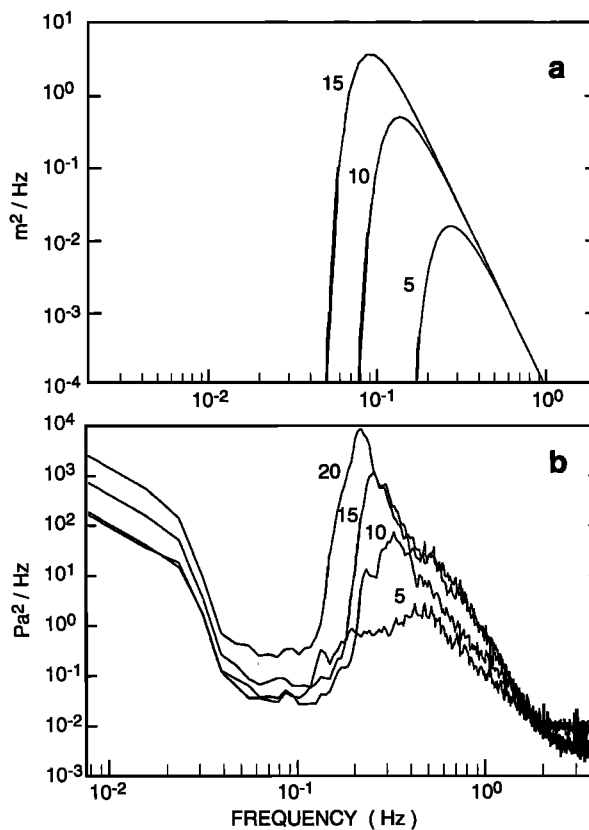


**Figure 10.** (top) Saturation ocean wave model spectra as a function of wind velocity meters per second. (bottom) Evolution of a seafloor pressure spectrum under a storm. Note the doubling of the peak frequency compared to the wind wave spectrum. From *Babcock et al.* [1994].

of ocean wave spectra [e.g., *Pierson and Moskowitz*, 1964; *Hasselmann et al.*, 1973; *Donelan et al.*, 1985]. These models follow an inverse power law at high frequencies (Figure 10) terminated at low frequencies below a spectral peak (at  $f_0$ ) by a precipitous falloff in energy. Wind wave height is determined by the wind velocity and the duration of a wind event or, if the duration is long, by the fetch. The fetch is the effective width of the storm, as waves eventually propagate out of the source region and therefore no longer evolve, or for basin scale wind fields it can be the entire width of the ocean basin. Winds of different velocity can produce a spectrum with a similar  $f_0$ , but the spectrum will evolve more quickly under a stronger wind. The shape of the spectrum is more peaked when the spectrum is quickly evolving, settling into a slowly evolving shape with a broader peak under steady winds [*Donelan et al.*, 1985].

The ocean wave height spectrum “saturates” at short periods. The energy in the wave height spectrum at a given frequency increases rapidly at first with increasing wind velocity up to a point after which increasing wind velocity leads to little increase in the energy in that wave component. Higher winds or a longer fetch put energy into the spectrum only at lower frequencies. The satu-

ration of the wave spectrum is evident in the envelope formed by the set of model wave spectra seen in Figure 10.

The saturation of the ocean wave spectrum suggests that microseisms derived from ocean waves should also saturate. *McCreery et al.* [1993] introduced this idea of a saturation spectrum to explain hydrophone data from the seafloor near Wake Island. They also suggested that the saturation spectrum should be constant worldwide, and they gave it a name: the “Holu” spectrum. The microseism spectrum saturates because of a balance between excitation by ocean waves and attenuation within the Earth [Webb, 1992]. In a lossless Earth the microseism amplitude would grow without bound as ocean waves continuously transferred energy to freely propagating elastic waves around the Earth.

A radiative transfer equation can be used to describe the excitation of microseisms within the waveguide formed by the large increases in seismic velocities with depth through the ocean, crust, and upper mantle [Hasselmann, 1963; Webb, 1992]. Energy travels primarily as Rayleigh waves in this waveguide. A minor component of the microseism wave field propagates as compressional or shear body waves or as Love waves [Haubrich and McCamy, 1969]. In general, theories for the prediction of microseism noise levels in the ocean that ignore the ocean floor waveguide underpredict the amplitude of the microseism peak by more than 20 dB. The radiative transfer equation models the energy in a wave field component along a ray path, taking into account excitation, dissipation, and changes in group velocity and divergence or convergence of ray paths. Predicting the microseism noise level at a site requires both a model for the coupling of ocean wave energy into elastic waves for a large area around the site, and an understanding of the propagation of microseisms within the Earth and ocean around the site. *Hasselmann* [1963] and *Webb* [1992] modeled the excitation of the primary Rayleigh wave components in the microseism wave field. The full steady state (saturation) microseism spectrum has been calculated for one Earth model by *Schmidt and Kuperman* [1989]. Modeling shows that the expected difference in the amplitude of the microseism peak between thinly sedimented and thickly sedimented areas is small (<10 dB) because the trapping and dissipation of the Rayleigh modes at 0.2 Hz is set by the deeper structure [Webb, 1992].

These studies ignore the effect of scattering of energy between modes, which may be important to setting the microseism noise level at the seafloor at short periods [Liu and Schmidt, 1993]. Scattering will tend to put energy into short-wavelength Stoneley and shear modes, for which the displacements are largest near the seafloor. The relative importance of scattering might be expected to be larger over thinly sedimented areas compared with thickly sedimented or un-sedimented regions, but the temporal variation in spectral levels of microseisms is large enough to have obscured any possible

variation due to differing geology in data sets published to date.

In large source regions such as under the trade winds the seafloor noise spectra approaches the Holu spectrum, which is the limiting result for an infinite source region. The lowest frequencies in the microseism peak never reach saturation, whereas the short-period waves are often close to saturation. The size of the source region required for the spectrum to be near to saturation is closely related to the attenuation  $e$ -folding scale for the dominant Rayleigh modes at a particular frequency in the microseism peak. Short-period microseisms saturate first but also attenuate quickly, so that they depend only on the local wind climate.

## 8. TEMPORAL AND GEOGRAPHICAL VARIATION OF MICROSEISMS

The ocean floor seismic noise spectrum depends on the wind and so varies with location and season. This section examines these variations to provide guidance for selecting potential sites for permanent ocean floor seismic observatories and for temporary deployments of ocean bottom seismometer arrays.

Long-period microseisms are always present because microseisms propagate long distances in the form of fundamental mode Rayleigh waves from any large storms over the oceans. For a Rayleigh wave, the  $e$ -folding scale for attenuation exceeds 5000 km at periods longer than 5 s, but this scale is small enough that there is a significant difference in the amplitude of the lowest-frequency microseisms (0.1–0.2 Hz) between the North Atlantic and Pacific seafloor (Figure 2). The North Atlantic Ocean is of limited fetch, so that even the most intense winter storms fail to develop the 20-s ocean waves needed to generate 10-s microseisms. Both the South Atlantic and Indian Oceans, however, are directly exposed to the long-period waves of the Southern Ocean.

At periods less than 5 s the  $e$ -folding scale for attenuation of Rayleigh modes is less than 5000 km, so that microseisms at a site are “regional” in the sense that these waves are driven mostly by waves (and hence wind) over the same ocean basin [Webb, 1992]. The  $e$ -folding scale is less than 100 km at periods shorter than 1 s, and because short-period ocean waves do not travel very far either, the sources of microseisms at higher frequencies are always very “local.” The dissipation timescale for 2-s ocean waves ( $e$ -folding time) is about 2.6 days, during which the waves propagate about 380 km [Lighthill, 1979]. Shorter-period waves dissipate more quickly and travel shorter distances.

The seafloor is usually noisy at 1 Hz because these microseisms are caused by 0.5-Hz (2-s period) ocean waves, and even a moderate breeze will quickly produce 2-s ocean waves. The timescale for the development of 2-s ocean waves is only about 2.5 hours under 5-m/s

winds or about 10 hours under 3-m/s winds [e.g., *Donelan et al.*, 1985]. The meteorology (wind) and rates of dissipation of ocean waves set the time and length scales of variations in microseism noise levels.

The short-period microseism noise level falls significantly only during periods of very light winds. Measurements from the seafloor of the Arctic Ocean in winter show what happens when the generation of microseisms is suppressed. The nearly continuous ice coverage prevents the excitation of ocean waves, so that the Arctic seafloor pressure noise levels in the microseism band are lower than the levels at any site yet measured in the Atlantic and Pacific Oceans [*Webb and Schultz*, 1992]. It is likely that the Arctic seafloor in winter provides some of the quietest seismic sites on Earth. Noise associated with motion of the ice becomes important at frequencies above about 10 Hz.

*McCreery et al.* [1993] have shown a strong correlation between wind speed and noise at 1 Hz at sites on the seafloor near Wake Island. The noise level near 1 Hz was on average 20 dB lower during calm conditions than when the wind exceeded 10 m/s. Above 10 m/s the noise level near 1 Hz increased only slowly with increasing wind speed, suggesting that the microseism spectrum was saturated. *Dorman et al.* [1993] also has shown that noise levels near 1 Hz can fall 20 dB during intervals of low winds. A record from the eastern Pacific over a period of 85 days shows several intervals of a few days with very light wind when the noise level at 1 Hz drops to low values (Figure 11). The noise level is 35 dB lower than typical values for several days during the second week of the record during an interval of glassy seas (no wind).

*Adair et al.* [1984] and *Hedlin and Orcutt* [1989] present the noisiest and quietest spectra from a compilation of seafloor vertical displacement spectra from various deep seafloor sites. The noise level at 1 Hz at the

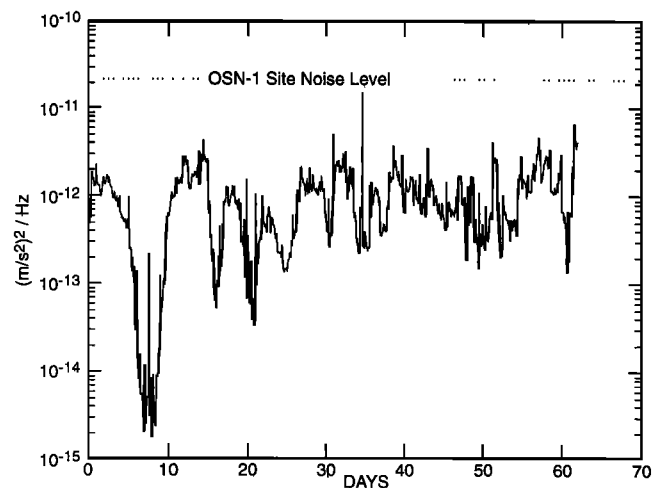


**Figure 11.** An 85-day record of acceleration spectral level near 1 Hz from a site near 9°N on the East Pacific Rise. The level seen at the OSN-1 site (from Figure 1) is also shown.

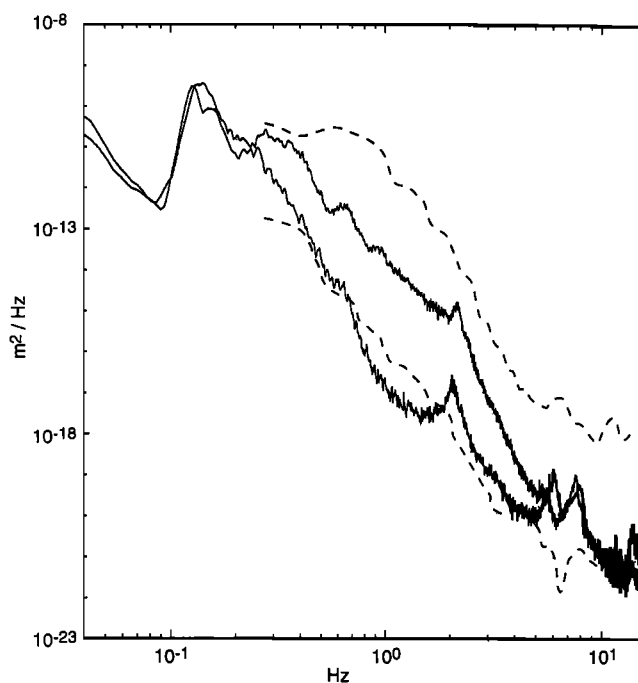


**Figure 12.** Noisy and quiet days from the East Pacific Rise (see Figure 11) plotted as a displacement spectra along with the noisiest and quietest spectra from a large series of OBS experiments from *Hedlin and Orcutt* [1989].

noisiest site was 40 dB above the quietest site. Figure 12 shows that one site can experience a similar range of conditions during a short interval.

The 35-dB variation in noise level seen in Figure 11 corresponds to a range of detection threshold at 30° range from  $m_b > 7.5$  to  $m_b < 5.5$  (Figure 7). During quiet periods the noise level at the seafloor is comparable to that at good terrestrial sites. For the purpose of detecting short-period, teleseismic body waves, one should seek sites where the wind is usually calm. Sites with strong, persistent winds are likely to be nearly useless for short-period measurements.

## 9. CLIMATOLOGY OF SHORT-PERIOD MICROSEISMS

A large range in noise levels has been reported for short-period microseisms at the seafloor [e.g., *Adair et al.*, 1984], but the geographical and temporal coverage of these reports is too spotty to provide much guidance toward situating permanent stations on the deep seafloor. It is difficult to know whether an OBS is correctly calibrated, so comparing published noise spectra is always uncertain. There is, however, a large statistical data set on winds over the world's ocean gathered by the U.S. Navy [*Naval Weather Service Detachment*, 1974–1979].

We can look for sites with long intervals of light winds as the most likely sites to provide quiet noise levels for permanent seismic observatories. The map in Figure 13

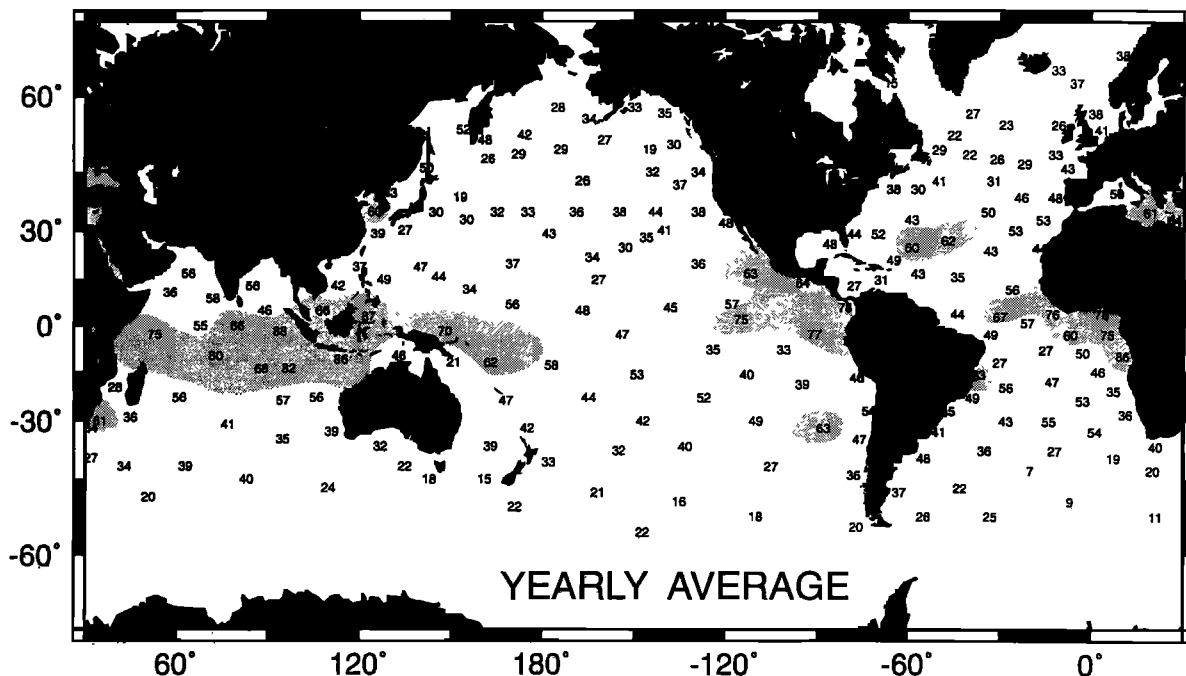


**Figure 13.** Yearly average of the percentage of reports when the wind at 10-m elevation was below 5 m/s. The shaded regions show areas where the wind was less than 5 m/s more than 60% of the time.

shows the fraction of time during an average year that the wind is less than 5 m/s at sites in all the oceans. In the shaded areas the winds are less than 5 m/s more than 60% of the time.

The 5-m/s contour is chosen because winds greater than 5 m/s are likely to generate 2-s ocean waves and therefore 1-s microseisms. The 5-m/s limit is supported by the Wake Island hydrophone data of *McCreery et al.* [1993]. Averaging the spectra in wind velocity bins, they found that noise levels near 1 Hz increased by 20 dB from calm to windy conditions and saturated at wind speeds exceeding 10 m/s. The 20-dB range at 1 Hz observed in the averaged data was much less than the total range of variation seen in the spectra from the experiment, suggesting that the averages are biased upward at low wind speeds and downward at high wind speeds by data from intervals when the wind was blowing over the hydrophone but not over the Wake Island site (where the wind was measured), and vice versa. Higher-frequency microseisms were found to saturate at lower wind speeds, as was expected. Noise levels at 2 Hz increased by about 12 dB over calm conditions and reached saturation at about 7-m/s wind speed. The wind speed values for saturation of the microseism spectrum are observed to be higher than would be predicted directly from simple models of ocean waves. This is probably because the excitation of microseisms also depends on the wind wave directional spectrum, which narrows toward the ocean wave spectral peak  $f_0$ . A stronger wind pushes the spectral peak toward lower frequency, broadening the directional spectrum and increasing the microseism level toward the saturation spectrum at short periods.

The main features in the contour map in Figure 13 would have been familiar to sailors centuries ago. The same features are evident in maps of mean wind speed derived from satellite altimeters [e.g., *Sandwell and Agreen, 1984; Challenor et al., 1990*]. Regions with frequent periods of light winds are expected to be relatively good sites for short-period seismology compared with typical ocean floor sites, while energetic sites will never provide low-noise observations. There are some obvious difficulties with using the Navy data to predict quiet sites. The level of error in ship observations of wind velocity is always high, and sites where the wind blows only during the day (calm 50% of the time), may still have a high microseism level because the ocean waves are not immediately attenuated.

The doldrums are a region of light winds that encircles the globe near the equator. In some parts of the equatorial South Atlantic and Indian Oceans, the wind is less than 5 m/s more than 75% of the time. The trade winds blow steadily in two bands between 10° and 20° to the north and the south of the equator. Intervals of light winds in the regions of the trades are relatively rare (<30%). A narrow region of lighter winds near 25°N and 25°S (the horse latitudes) separates the trade winds from the westerlies. In general, the Atlantic and Indian Oceans see lighter winds than does most of the Pacific. Finally, the strong winds in the great Southern Ocean (the roaring 40s and screaming 50s) are obvious from the rarity of intervals of light winds at latitudes south of 40°S.

Not unexpectedly, there is a strong seasonal cycle to the probability of light winds at most sites (Figure 14). The winds are lighter in the northern hemisphere during the northern summer (June–August) and lighter in the

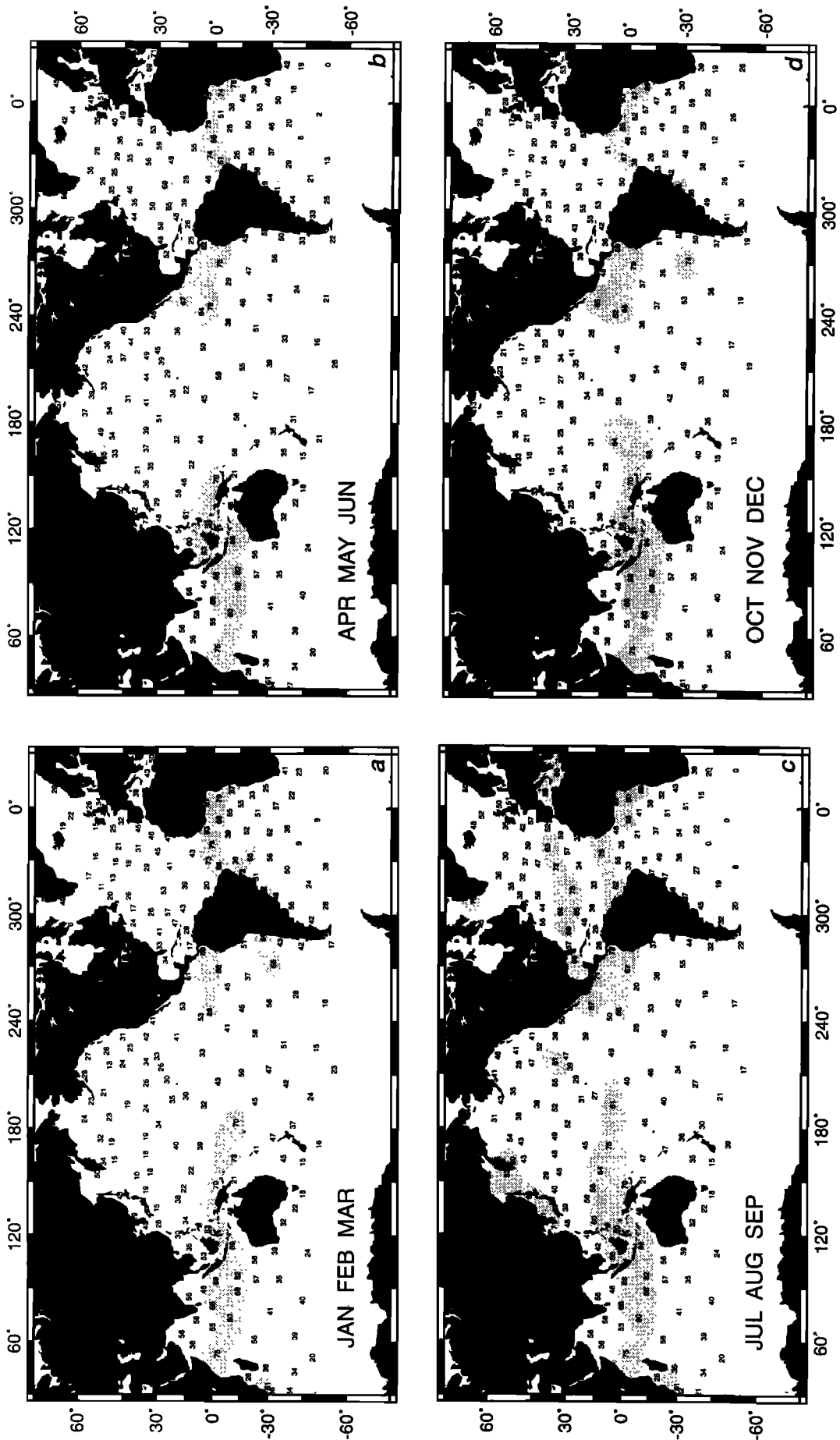


Figure 14. Seasonal averages of the percentage of reports when the wind at 10-m elevation above the sea surface was below 5 m/s. The shaded regions show areas where the wind was less than 5 m/s more than 60% of the time.

southern hemisphere in the southern summer (November–February). A large area of light wind appears in the north central Atlantic Ocean during the summer, suggesting that low noise levels are to be found in summer in the North Atlantic. A large area of light winds is also found in the equatorial Atlantic and Indian Oceans in fall and spring. Parts of the western equatorial Indian Ocean are windy in the summer because of the monsoon. There are no significant areas of low wind in the northern Pacific, other than on the equator near the Galapagos Islands, and the western southern Pacific appears to occasionally offer quiet sites for short-period seismology.

There is a need for a systematic investigation of short-period noise levels with location on the seafloor. The contours maps in Figures 13 and 14 are designed to provide a guide for planning permanent stations and for planning long temporary OBS deployments. The *Blackman et al.* [1995] study and our own experience with many experiments using OBSs in the Pacific confirm that it is unusual to detect short-period arrivals from teleseismic earthquakes because so much of the Pacific is windy and therefore noisy. The central Atlantic near 35°N, 35°W, is often calm (72%) during early summer (Figure 14c) where short-period arrivals from distant earthquakes in South America with  $M_s < 5.6$  were recorded [Forsyth, 1996]. The Indian Ocean near 25°S, 70°E, is usually calm (80%) during the month of August (Figure 14c) and there too, short-period arrivals were seen from six teleseismic earthquakes during a 3-week period [Sato *et al.*, 1996].

## 10. SHORT-PERIOD NOISE IN BOREHOLES INTO THE SEABED

Seismometers are installed in boreholes on land primarily to escape long-period noise associated with the local deformation of the ground under short-wavelength atmospheric pressure fluctuations. Ocean currents are a similar source of noise at the seabed, but shallow burial of the sensors is sufficient to attenuate short-period flow noise to negligible levels. There have been a series of experiments investigating noise levels in boreholes in the seabed. The primary goals of these experiments have been to improve the signal to noise ratio for short-period signals and to improve sensor coupling to the seabed.

As was shown earlier, the detection limit for teleseismic, short-period arrivals can be greater than  $7.5 m_b$  at many seafloor sites. Any improvement that can be obtained in signal to noise ratios in this band will greatly improve the utility of a seismic station. Energy is coupled from ocean waves into acoustic waves and then into elastic waves below the seabed to form the microseism peak in seafloor spectra. The wavelength of a 1-Hz acoustic wave in the ocean is 1.5 km, and the wavelengths of the Rayleigh wave modes below the seabed are even larger. Installing sensors at depths as great as several hundred meters will not necessarily ensure better

signal to noise ratios for short-period signals because of the large vertical scales associated with these modes. Significant reduction in noise levels might not be expected until depths of several kilometers are reached, beyond the present range of ocean drilling.

Some improvement in SNR is expected at shallow depths because some microseism energy is scattered by bathymetry and by topography on the sediment-seabed interface into short-wavelength shear modes. Finite difference models of wave propagation demonstrate that energy readily couples from acoustic waves into short-wavelength modes during interaction with a rough bottom [Dougherty and Stephen, 1991; Liu and Schmidt, 1993; Stephen and Swift, 1994; Bradley and Stephen, 1996; Bradley *et al.*, 1997]. The slowly propagating shear (Stoneley) modes are trapped to the sediment-water interface with displacements that decay away from the seafloor with an  $e$ -folding constant proportional to wavenumber. An experiment to detect short-wavelength components of ocean floor noise using a small-aperture array of OBSs demonstrated coherence falling rapidly with horizontal separation of the sensors. Correlation lengths were 100–200 m at frequencies above 0.4 Hz [Schreiner and Dorman, 1990]. This result requires significant energy in short-wavelength waves.

Several experiments have been conducted to study the short-period noise level in boreholes into the seabed. Carter *et al.* [1984] found vertical noise levels only 3–8 dB lower in the band from 2 to 10 Hz on a sensor clamped at a depth of 194 m below the seafloor in Deep-Sea Drilling Project (DSDP) Hole 494A off Guatemala, compared with ocean bottom seismometers placed near the hole. A second experiment in the northeast Pacific with the seismometer clamped deeper in the borehole (and below the sediment layer at 378 m) found lower noise levels between 4 and 15 Hz were 15–25 dB below nearby ocean bottom seismometers [Duennebier *et al.*, 1989]. Signal levels were reduced by the higher impedance in the basalt than in sediment, so the resulting signal to noise ratios on the vertical component for arrivals from one large distant earthquake were only a few decibels better at 2–10 Hz and 10 dB better at higher frequencies. The improvement in signal to noise ratio for short-period arrivals on the single horizontal component was about 10 dB.

Borehole experiments that have studied noise below 1 Hz have found that the difference between seafloor and borehole noise levels increases rapidly with frequency. An experiment in the tropical western Pacific (DSDP Hole 395A) found vertical noise levels for a seismometer at 516-m depth only 10 dB lower at 0.2 Hz but 28 dB lower at 2 Hz [Adair *et al.*, 1984]. The authors concluded that these data were consistent with noise propagating as fundamental mode Stoneley waves between 0.2 and 2 Hz. A similar experiment in the Sea of Japan with a seismometer at 715-m depth found noise levels similar to those at Hole 395A in the band from 0.3 to 10 Hz but atypically low levels between 0.1 and 0.3 Hz, presumably

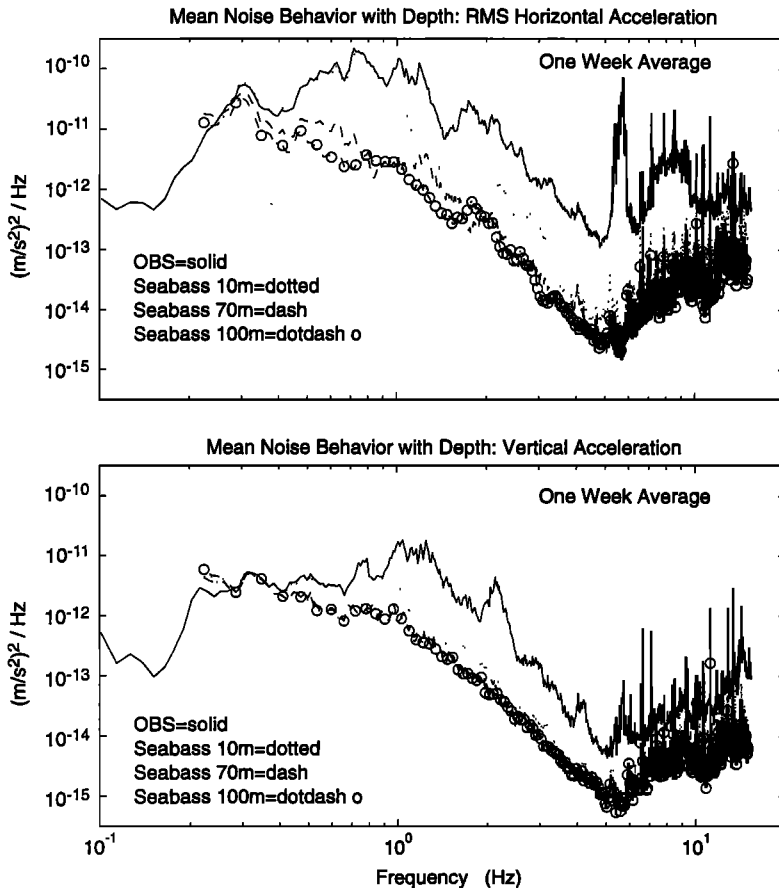


**Figure 15.** (top) Horizontal and (bottom) vertical noise spectrum from a North Atlantic site on the seafloor and at 10, 70, and 100 m below the ocean floor in Deep-Sea Drilling Project borehole 534B [from *Bradley et al.*, 1997].

because this site was shielded by its location in the Sea of Japan [*Suyehiro et al.*, 1995]. *Hedlin and Orcutt* [1989] found a similar shift in the microseism peak toward higher frequencies on the island of Taiwan compared with other Pacific island sites.

Data from seismometers locked at three depths in a borehole near the Bahamas show how short-period noise decreases with depth and as a function of frequency [*Stephen et al.*, 1994; *Bradley et al.*, 1997]. The difference between the vertical noise level at 1 Hz on the seafloor and at depth increases from 6 dB at 10-m depth to 10 dB at 100-m depth (Figure 15). At higher frequencies the vertical spectra from the borehole sensors at 10-, 70-, and 100-m depth differ by less than 3 dB but are 10–15 dB quieter than spectra from the seafloor. On the horizontal components the decrease in noise levels is larger, reaching 15 dB at 70-m depth at 1 Hz and 20 dB at higher frequencies. Most of the improvement occurs in the first 10 m for frequencies above 1.5 Hz, but below 1 Hz the sensor at 10-m depth was only a few decibels quieter than the seafloor sensor. The depth dependence at 0.3 Hz was consistent with propagation as fundamental mode Rayleigh waves with little difference in vertical and horizontal component noise levels between the seafloor and borehole sensors.

The results from the several borehole experiments to date are consistent. Vertical noise levels are lower within the basement rocks (10–15 dB at 1 Hz, increasing to 20

dB at about 5 Hz). Signal levels are also smaller (because of changing impedance), so that the resulting improvement in signal to noise ratio is near zero at 0.2 Hz and increases to more than 10 dB at a few hertz. For the horizontal components the improvement is much larger and occurs mostly within the upper 10 m. These improvements in signal to noise ratio are obvious in the different structure of the borehole and ocean bottom noise spectra (Figure 15). The deep spectra closely follow a power law dependence on frequency with a slope of 80 dB/decade [*Adair et al.*, 1984]. In contrast, surface spectra show significant peaks in the band around a few hertz associated with the Stoneley or shear modes. The horizontal and vertical spectra at depth differ by only a few decibels consistent with propagation of the microseisms as Rayleigh waves.

The improvements in signal to noise ratio for sensors at shallow depths in boreholes (>10 mbsf) should lower detection thresholds for short-period body waves from  $7.5 m_b$  expected for noisy seafloor sites (saturated microseism spectrum) to about  $6.5 m_b$  (Figure 7). Detection limits for quiet seafloor noise conditions are expected to fall below  $5.5 m_b$ . *Butler and Duennebier* [1989] report on teleseismic earthquakes recorded by a borehole seismometer during a 2-month recording period that included 15 nuclear explosions. Only the largest nuclear blast ( $5.6 m_b$ ) was recorded. The authors note the importance of the high frequencies (6.5-Hz *P*

wave) present in the blast seismogram in the detection of this event. This large blast was observed during a quiet period, after which noise levels were higher. The authors believe that smaller events might have been observed had noise levels continued at the low level. The smallest earthquake observed was  $5.4 m_b$ ; all other teleseismic earthquakes seen were greater than  $6 m_b$ . The station was on old oceanic crust with correspondingly low attenuation in the lithosphere, so that high-frequency  $S$  waves were observed from regional events.

*Orcutt and Jordan* [1986] report on detection thresholds from the deployment of a borehole seismometer in the western Pacific [*Adair et al.*, 1984]. The detection limit for this site increased from  $m_b \approx 5.2$  at a distance of  $40^\circ$  to  $m_b \approx 5.6$  at  $80^\circ$ . The instrument was near  $25^\circ\text{S}$ ,  $165^\circ\text{E}$ . During February at this site, the wind is expected to be less than 5 m/s more than 73% of the time (Figure 14a), suggesting that noise levels should be low near 1 Hz. Wind speeds observed from the ship above the borehole were mostly less than 5 m/s during the relevant interval. The low detection threshold observed is consistent with the low noise model in Figure 7, particularly if the observations are associated with deep earthquakes from the subduction zones of the western Pacific, with signals propagating along low attenuation paths (small  $t^*$ ). Regional earthquakes could be detected at a still lower threshold ( $m_b = 4.6$ ) because of energy propagating as  $P_0$  waves in the high  $Q$  lithosphere.

Borehole installation can provide a small but significant improvement in signal to noise for short-period arrivals compared with seafloor installations. The improvement is less than 10 dB for vertical component measurements and 10–15 dB for horizontal sensors corresponding to 1–1.5 units of magnitude in detection threshold. The one measurement of depth dependence suggests that all improvement in signal to noise ratio occurs in the first 50 m. This result is consistent with observations of short correlation scales for sensors on the seafloor [*Schreiner and Dorman*, 1990], and with significant propagation of noise in short-wavelength Stoneley modes. Others have argued that the depth dependence simply reflects noise coupled into the top of borehole at the exposed reentry cone propagating down the upper 50 m of poorly cemented casing (F. K. Duennebie, personal communication, 1997). For short-period measurements there do not appear to be significant advantages to drilling much deeper or significant differences between installation in rock rather than sediments. The role of borehole installation for long-period measurements is described in section 20.

## 11. OCEAN FLOOR CURRENTS AND SHORT-PERIOD NOISE

At one time the deep ocean was thought to be essentially quiescent, but measurements have demonstrated that currents can sweep some parts of the deep ocean

floor with speeds as high as 75 cm/s [*Rhines*, 1977; *Gross et al.*, 1986]. The largest velocities are found under the western boundary currents along the western edge of each basin [*Rhines*, 1977]. Currents can also be large around bathymetric features such as deep-sea canyons or the tops of seamounts [*Brink*, 1995]. Currents are enhanced at the top of mid-ocean ridges [*Allen and Thomson*, 1993] and through narrow sills [e.g., *Lonsdale*, 1977]. However, at most places on the deep seafloor away from the western boundary, the currents are mostly weak, rarely exceeding 10 cm/s and less than 5 cm/s at many sites. Currents in shallow water (such as on the shelf) tend to be much higher [e.g., *Gross et al.*, 1992].

Currents as small as 10 cm/s can produce significant short-period noise on both vertical and horizontal components of poorly designed ocean bottom seismometers [*Duennebie et al.*, 1981]. Narrow and tall ocean bottom seismometers are particularly susceptible to bottom currents. Usually, the spectrum of current induced noise is “red” with much higher spectral density at long periods. Radio antennas and other small elements such as taut cables have been observed to “strum” in the current, producing narrow, energetic peaks in the noise spectrum at frequencies of a few hertz. The short-period current noise problem has been studied by *Trehu* [1985b], and *Kasahara et al.* [1980]. All recent designs for short-period instruments [e.g., *Trehu and Sutton*, 1994; *Sauter et al.*, 1990] have isolated the inertial sensors in small pressure cases that are deployed separately on the seafloor at a distance of about 1 m from the main recording package. This allows for a low, compact, sensor package that is less affected by the direct action of current, although current-induced recording package motion may perturb the sensors by coupling through the ground [*Duennebie and Sutton*, 1995].

Currents stronger than 10 cm/s increase short-period noise levels even on low-profile instruments. The energy in the current-induced pressure fluctuations varies as the fourth power of the velocity (Figure 16). *Trehu* [1985b] found the same power law for short-period seismic noise on an OBS. On land it is usual practice to dig a hole for any temporary installation of a seismometer so that the seismometer is well coupled to the ground, and out of the wind. *Trevorrow et al.* [1989] and *Duennebie et al.* [1991] have demonstrated the utility of shallow burial in high-current coastal environments for improving sensor coupling and avoiding flow-induced noise on the seabed. Borehole installation will also shield sensors from the effects of ocean currents, but sensors can be affected by circulation in the borehole driven by the geothermal gradient. This is a particular problem for long-period measurements and is discussed later.

## 12. LONG-PERIOD NOISE SUMMARY (<0.1 HZ)

There have been few long-period measurements of seafloor noise using seismometers. Most of the pub-

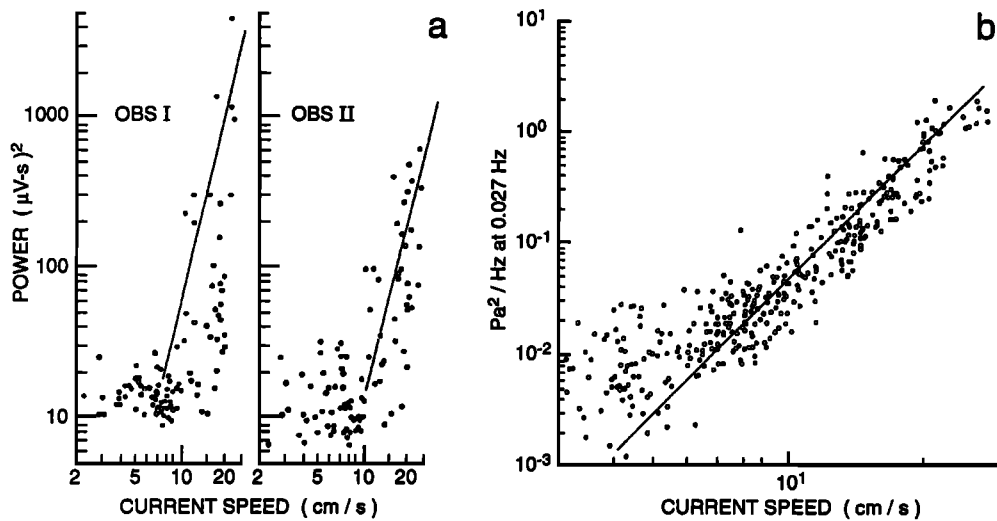


**Figure 16.** (left) Measured noise levels (vertical velocity) from two OBSs at 2–5 Hz versus current speed. Noise levels rise as the current velocity to the fourth power, if the current exceeds 10 cm/s [from *Trehu*, 1985]. (right) Measured noise level in pressure at 0.027 Hz versus current speed (from *Webb* [1988]; © 1988 IEEE).

lished observations are shown in Figures 1 and 17. *Crawford et al.* [1991], *Webb et al.* [1994], and *Sutton and Barstow* [1990] show measurements of the long-period acceleration spectra from the Pacific, and *Beauduin and Montagner* [1996] show measurements from the North

Atlantic. There are many long-period pressure measurements from the Pacific, Atlantic, and Arctic Oceans using differential pressure gauges (Figure 2).

As on land, the noise levels at the seafloor fall precipitously below the microseism peak at 0.2 Hz (Figures 1 and 17). Long-period noise levels on the seafloor are controlled either by ocean currents or by the effects of low-frequency ocean waves. These sources are absent from continental sites, although ocean currents have an analog on land in the form of wind. At frequencies below 0.03 Hz, infragravity waves in the Pacific raise noise levels in the pressure spectrum by 40 dB compared with higher frequencies. The resulting deep trough between the infragravity waves and the microseism peak in the pressure spectrum is sometimes called the noise notch (Figure 2). The noise notch in the pressure spectrum and the low noise levels seen in the vertical acceleration spectrum below the microseism peak allow the detection of body waves from moderate size earthquakes ( $M_w > 5.5$ ) at teleseismic ranges ( $>30^\circ$ ) at sites almost anywhere on the seafloor. Although horizontal component noise levels rise rapidly at low frequencies because of tilt noise, it is also usually possible to detect shear waves from moderate earthquakes with these sensors at frequencies just below the microseism peak.

The pressure signal decays exponentially away from the sea surface under an ocean wave with an  $e$ -folding constant equal to the wavenumber of the ocean wave. Waves at frequencies above 0.03 Hz are too short in wavelength to be seen on the deep seafloor. Long-period vertical acceleration noise levels driven by deformation under infragravity waves depend on the shear strength of the oceanic crust. Vertical component seismometers provide better signal to noise for long-period seismic measurements than do pressure sensors because the effects of the infragravity waves are relatively smaller.

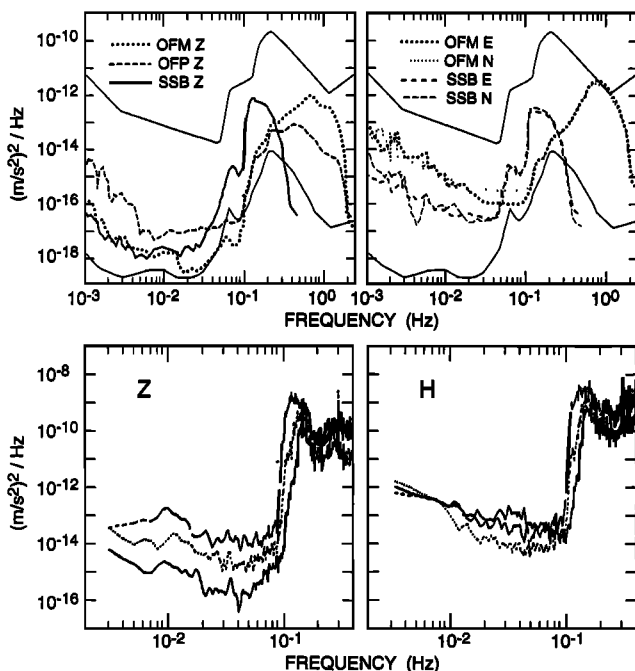


**Figure 17.** Long-period spectra (top) from a borehole sensor (OFP) and a seafloor sensor (OFM) in the eastern North Atlantic [*Beauduin and Montagner*, 1994] and (bottom) from the eastern North Pacific (reprinted with permission from *Sutton and Barstow* [1990]; copyright 1990 Acoustical Society of America). Vertical components are labeled “Z”; horizontal components are labeled “H” or “E” and “N.” The thin lines on the top panels show the high and low noise continental site models.

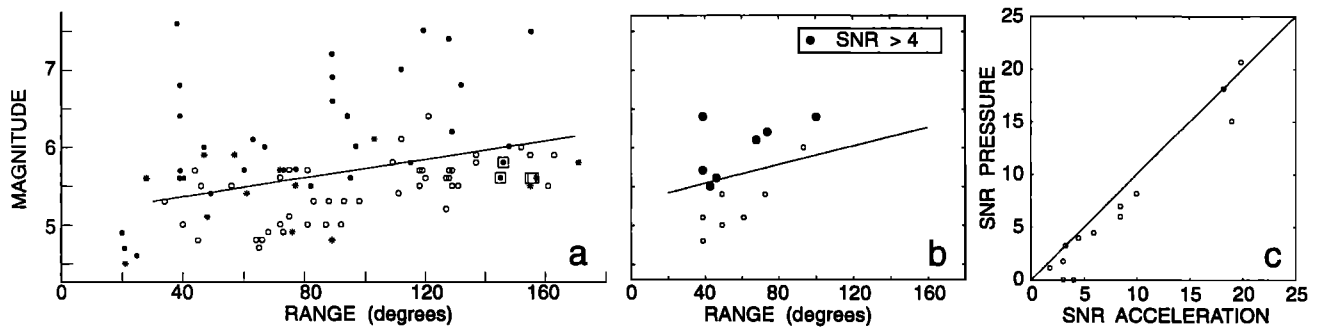


**Figure 18.** (a) Long-period  $P$  waves detected with a pressure gauge versus range [Blackman *et al.*, 1995]. Solid dots represent events with observable  $P$  waves. (b) Long-period  $P$  waves detected at the OSN-1 site versus range using a broadband vertical instrument [Webb *et al.*, 1994]. Solid dots have signal to noise ratio (SNR) greater than 4. (c) SNR (in decibels) for  $P$  waves observed using the differential pressure gauge versus SNR using the vertical long-period seismograph.

The amplitude of the infragravity wave field is directly related to the short-period ocean wave climate around the perimeter of an ocean basin. Infragravity wave energies are high in the Pacific and vary little over time. North Atlantic infragravity wave amplitudes vary from day to day by more than 30 dB but reach Pacific levels only during large storms. During quiet intervals the vertical acceleration noise below the microseism peak at sites on the seafloor in the North Atlantic can be as quiet as that at good continental sites (Figure 17). The Arctic seafloor is known from pressure measurements to be very quiet at low frequencies during the winter, when it is covered by the icecap (Figure 2), suggesting that the vertical acceleration spectrum during winter should be comparable to the low-noise spectrum from the North Atlantic. Long-period noise levels at Indian Ocean and South Atlantic sites are unknown but are likely to be high because of the energetic wave climate in the Southern Ocean, and spectra should resemble noisy North Pacific spectra (Figures 1 and 2).

Horizontal component noise levels at 100-s period can exceed vertical noise levels by 30–60 dB for instruments on the seafloor (Figure 17) because the instruments rock slightly under ocean currents (tilt noise). The acceleration of gravity is rotated into the horizontal components, producing large apparent accelerations even for very small tilts. Tilt noise can also affect the vertical noise levels if the sensor is not precisely aligned with the local vertical. Tilt noise is less of a problem on land because seismometers are usually buried or installed in vaults or boreholes rather than dropped onto soft sediments. Significant improvements in horizontal noise level have been obtained by burying the sensors just below the seafloor in the sediments at continental shelf sites. Horizontal component data from deep-sea borehole installations as of yet have been noisy, probably because of circulation within the water-filled borehole.

Rayleigh waves can be observed from moderate earthquakes using both pressure sensors and vertical component long-period seismometers below the micro-

seism peak, but inertial sensors provide better records because of lower noise from infragravity waves. During quiet intervals in the North Atlantic and on the Arctic seafloor during winter, it should be possible to measure Rayleigh wave dispersion to 200-s period and to measure the Earth normal mode eigenfrequencies with vertical component seismometers. Teleseismic Love waves were detected with OBSs with useful signal to noise ratios from two Pacific earthquakes during the Mantle Electromagnetic and Tomography (MELT) experiment [Forsyth, 1997].

### 13. DETECTION LIMITS FOR LONG-PERIOD BODY WAVES

The low noise levels in the noise notch between 0.03 and 0.1 Hz (periods of 10–30 s) make it possible to detect long-period (10–50 s) body waves from earthquakes with magnitudes as small as  $M_w = 5.5$  at teleseismic distances ( $>30^\circ$ ) with either seafloor pressure or inertial measurements. The best signal to noise for body waves occurs at frequencies near 0.06 Hz (17-s period), just below the single-frequency microseism peak.

Blackman *et al.* [1995] have compiled pressure records from 11 recent experiments using ocean bottom sensors to study the detection threshold for long-period  $P$  waves. The study took the larger of the  $M_s$  magnitude and the  $m_b$  magnitude as a measure of the size of an earthquake. The relationships between  $m_b$ ,  $M_s$ , and  $M_w$  are discussed in the appendix. The detection limit increased from  $M_s = 5.5$  at  $40^\circ$  range to  $M_s = 5.9$  at  $100^\circ$  range (Figure 18). Similar phases (e.g.,  $PKP$ ) exhibited comparable detection thresholds at comparable ranges. The noise floor for the differential pressure gauges (DPGs) used in these measurements is controlled by instrument noise, so better technology could provide lower detection thresholds for long-period body waves.

The records from the 1-Hz geophones (Mark Products L-4) used in most of the instruments in the U.S.

OBS fleets are noisy at long period because of rapidly rising electronic noise levels. Most OBSs use standard operational amplifiers [Riedesel *et al.*, 1990] which establish instrument noise levels that are just above ground noise on the vertical component at 10-s period, but that rise to more than 60 dB above the true seafloor noise level at 100-s period (Figure 6). Considerably better amplifiers can be built which could provide noise floors nearly comparable to ground noise to periods as long as 100 s using these same 1-Hz sensors. Newer OBSs will therefore have lower longer-period noise levels, but most OBS today are sufficiently quiet to allow the detection of long-period body waves in the band between 10 and 20 s with only slightly poorer signal to noise ratio than true broadband instruments.

Only a small number of earthquakes have been recorded by true broadband or long-period inertial sensors deployed on the seafloor. The data in Figure 19 are from a seafloor instrument that uses a LaCoste-Romberg gravimeter similar to the sensors used in the International Deployment of Accelerometers (IDA) network [Agnew *et al.*, 1986] as a vertical component seismometer [Webb *et al.*, 1994; Crawford *et al.*, 1991]. The instrument also carries a DPG. The low-pass-filtered DPG record looks nearly identical to the record from the vertical accelerometer. The phase relationship between the sensors is similar because a single pole in the pressure electronics near 10-s period makes the output proportional to the time derivative of pressure rather than to pressure. The records are not identical, however. The most important difference is that the body waves appear to arrive 2 s earlier in the DPG pressure record than in the vertical acceleration record. This result is not due to differences in the instrument response but rather occurs because the waveforms are perturbed differently by interference between the direct arrival and water column reverberations hidden by the low-pass filtering needed to detect the long-period arrivals. Long-period arrivals are best measured with acceleration sensors, as is discussed in the next section.

During a 20-day deployment of this long-period vertical seismometer at the OSN-1 site south of Hawaii, 14 earthquakes were seen with clear body wave arrivals [Webb *et al.*, 1994]. The smallest of these earthquakes was a  $M_s = 5.4$  event at a distance of  $43^\circ$ . The signal to noise ratios were slightly better for arrivals on gravimeter records than on DPG records from the same site (Figure 18). Detection limits increased slightly with range for both pressure and vertical acceleration measurements following the Blackman *et al.* [1995] model. The models for signal and noise in Figure 7 are in good agreement with the signal to noise ratios seen in Figure 18.

Vertically polarized shear waves are converted to compressional waves at the seafloor or at the base of the sediments and are detected in long-period seafloor pressure or vertical component acceleration records from moderate earthquakes (Figure 19). The shear wave arrivals are usually slightly larger in amplitude than the

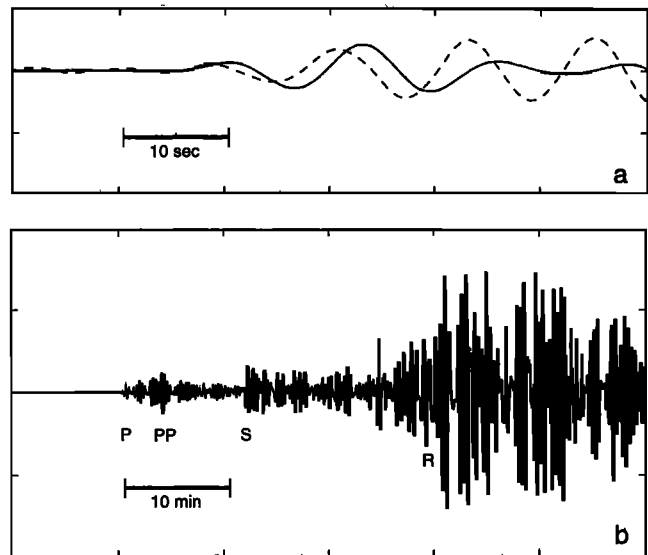


**Figure 19.** (top) Filtered (10–30 s) record of pressure (dashed) and vertical acceleration (solid) from an Indonesian event recorded at the OSN-1 site south of Hawaii. Note that the pressure  $P$  wave arrival appears to lead the acceleration arrival by about 2 s. (bottom) A longer acceleration record from the same event.

compressional arrivals and so should be recorded any time long-period  $P$  waves arrivals can be seen. Only long-period shear wave arrivals (other than  $S_0$ ) are ever seen at teleseismic distances because strong attenuation removes the short-period energy at frequencies above the microseism peak.

It is important to also record horizontally polarized shear waves to obtain measurements of shear wave splitting. Horizontal component noise levels can be as much as 40 dB higher at 20-s period than vertical component noise levels (Figure 17). Despite high long-period noise levels, there is usually a band between 10-s and 20-s period of sufficiently low noise level to record teleseismic  $SH$  arrivals from large earthquakes during quiet intervals using either short-period or long-period sensors. During noisy intervals, or at noisy sites, detection thresholds for long-period body waves on horizontal component sensors can be so high as to make the horizontal components useless for seismology.

#### 14. REVERBERATION PROBLEM FOR LONG-PERIOD BODY WAVES

Teleseismic, long-period body wave arrivals can be routinely detected on the seafloor using either pressure or inertial sensors because of the low noise levels in the noise notch, but a multipole low-pass digital filter must be applied before the arrivals can be clearly seen above the energetic microseisms. These filters limit the rise time of arrivals to many seconds (Figure 19), so unless the signal to noise ratio is extremely large, it is impossi-

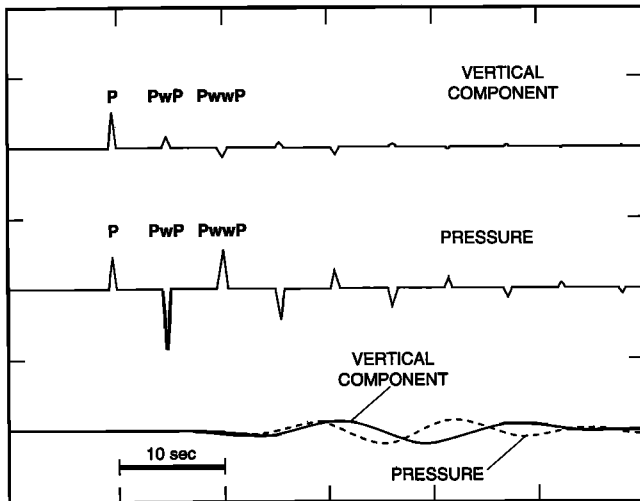


**Figure 20.** Model of the  $P$  wave arrival and subsequent reverberations ( $PwP$ ,  $PwwP$ , etc.) for a seabed site at 4-km depth, shown unfiltered and filtered. The filtered pressure arrival appears to arrive 2 s before the acceleration arrival.

ble to pick the first motion with an accuracy much better than 1 s. A cross-correlation technique is usually applied to sections of filtered data to best resolve the relative arrival times between stations [e.g., *Blackman et al.*, 1993].

Water column reverberations complicate the analysis of long-period body waves by interfering with the shapes of the arrivals. The apparent arrival times shift with the water depth, as the phase of the interference depends on the travel time through the ocean. *Blackman et al.* [1993, 1995] found that arrivals at stations directly on the axis of the Mid-Atlantic Ridge were about 0.5 s earlier than arrivals off axis, the result of increasing depth away from the axis. The problem is similar to the effect of water column bounces on the long-period waveforms of undersea earthquakes observed at teleseismic distances. The effect of these reverberations on waveforms has been studied as part of the problem of determining earthquake depths [e.g., *Stein and Wiens*, 1986; *Hermann*, 1976; *Ward*, 1979]; for example, waveforms are affected by the sloping bathymetry near the source for subduction zone earthquakes [e.g., *Okamoto and Miyatake*, 1989; *Wiens*, 1989]. Converted and reflected phases from interfaces other than the seafloor and sea surface [e.g., *Lewis and McClain*, 1977] might also have a small effect on arrival waveforms.

*Blackman et al.* [1995] describe the reverberation problem and the dependence of the apparent arrival time on filter bandwidth and water depth for narrow-band, symmetric (acausal) filters. The figures in this paper differ from *Blackman et al.*'s in the use of causal filters to avoid precursors to the true first arrival, but in either analysis the filtered  $P$  wave pressure waveform appears to be shifted early relative to the acceleration waveform for most water depths.

Any  $P$  (or  $PKP$ ,  $PP$ ,  $SP$ , etc) wave phase incident from below at the seafloor will be transmitted through the interface with a transmission coefficient of about 0.7 [*Blackman et al.*, 1995]. The upgoing  $P$  wave in the water reflects at the sea surface with a reflection coefficient of  $-1$ . The downgoing, negative (in pressure) reflected  $PwP$  wave meets the original positive upgoing  $P$  wave at the seafloor after a two-way travel time delay of about 4 s. This sequence of arrivals is modeled as a string of pulses in Figure 20. The actual shape of the pulses affects the modeling of the filtered arrivals only slightly, since the pulse length is usually short compared with the rise time of the filters. The downgoing reflected  $PwP$  wave reflects on reaching the seafloor with a positive reflection coefficient of 0.7, so the amplitude of the pulse associated with the  $PwP$  phase at the seafloor is  $-1.7$  times as large than the initial  $P$  wave arrival in the pressure record. The surface-reflected pulse in acceleration is in phase with the original incident wave, and the seafloor reflection coefficient is negative so that the observed  $PwP$  phase is only 0.3 times as large as the incident wave when observed with a vertical acceleration sensor. The smaller, noninverted  $PwP$  arrival in the acceleration record sums with the incident  $P$  wave but produces little change in the apparent arrival time in a filtered record.

In short-period records the  $P$  and  $PwP$  phases are observable as separate arrivals. In long-period, filtered records the reverberations merge with the original wave and appear as a single arrival with an arrival time that depends on the time delay between the reverberations [Figure 20]. Each pulse is convolved with the filter response, becoming a series of oscillations with a period corresponding to the high-frequency corner of the filter. For this low-pass-filtered record the maximum amplitude in the  $P$  wave is not reached until after more than 25 s. The first motion appears to be delayed by 9 s in the acceleration record and by about 7 s in the pressure record, so that the arrival appears to come in 2 s earlier in the pressure record. In reality, the two arrivals are simultaneous.

The filter pass band and the local bathymetry determine the apparent relative delay between the pressure and acceleration waveforms. *Blackman et al.* [1995] explored the effect of water depth on the relative arrival time in pressure records. Changing the water depth from 2.2 to 3.5 km was found to advance or retard the apparent arrival time in pressure over a range from  $-0.5$  to  $+1.5$  s depending on the filter. Figure 21 shows similar results for the  $P$  wave at the seafloor in water from 3 to 6 km deep observed in pressure and vertical acceleration. The pressure record mimics the *Blackman et al.* [1995] result, showing a large shift in the apparent arrival time with water depth. In contrast, water depth has only a subtle effect on the apparent arrival time in the acceleration record. Long-period body wave arrivals are thus more directly and accurately determined using vertical seismometers.

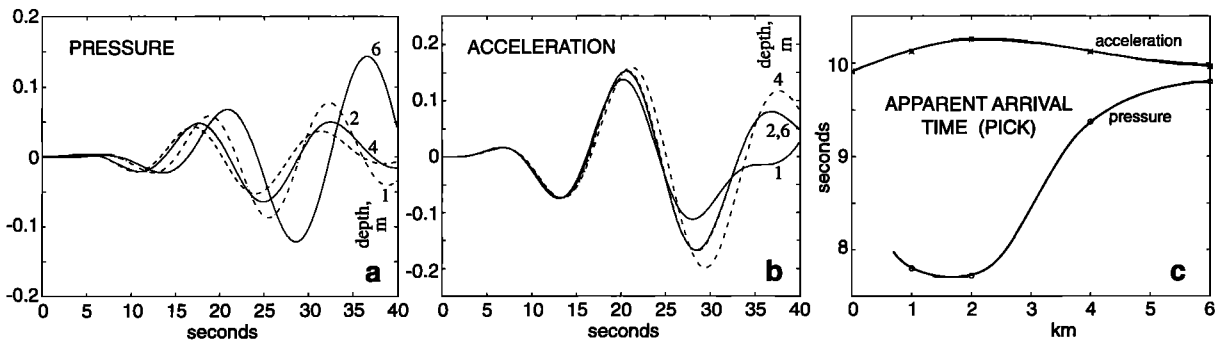


**Figure 21.** Models of  $P$  wave arrivals at the seafloor for water depths from 1 to 6 km depth, filtered from 0.03 to 0.08 Hz, for (a) pressure and (b) vertical acceleration, and (c) apparent arrival time (pick) versus depth for model arrivals taking 20% of the first oscillation as the likely pick point in noisy data for both pressure and vertical acceleration.

## 15. DETECTION LIMITS FOR NORMAL MODES AND SURFACE WAVES

The largest amplitude and best signal to noise ratio in a surface wave train occurs at periods near 20 s. The earthquake magnitude scale  $M_s$  is based on the amplitude of 20-s Rayleigh waves (see appendix). The spectra of Rayleigh or Love wave wavetrains vary greatly with the source mechanism and depth of the earthquake [Aki and Richards, 1980], with shallower earthquakes typically generating more short-period surface wave energy. A model for Rayleigh wave amplitudes in one-third octave bands in vertical acceleration is shown for earthquakes with moment magnitudes ranging from  $M_w = 6$  to  $M_w = 8$  in Figure 7a [from Agnew *et al.*, 1986].

The pressure signal associated with a Rayleigh wave depends on the water depth, as the air-sea surface is essentially a pressure release surface. The ratio of the pressure to vertical acceleration at the seabed in a Rayleigh wave is  $p/a = -\rho/r \tan(rH)$ , where  $H$  and  $\rho$  are the water depth and density and  $r$  is the vertical wavenumber. For low frequencies,  $rH \ll 1$ , so that the ratio of pressure to acceleration becomes  $p/a \approx -\rho H$ . The Agnew *et al.* [1986] model curves are recalculated for pressure at the seafloor in 4-km water depth in Figure 7b.

Rayleigh waves can begin to be detected near 20-s period at teleseismic ranges at Pacific seafloor sites from earthquakes with magnitudes larger than  $M_s \sim 5$ . The detection of longer-period waves requires larger earthquakes. Models of Earth structure are derived from measurements of wave dispersion. The signal to noise ratio is the limiting factor to the accuracy of phase velocity ( $C$ ) measurements:

$$\frac{\Delta C}{C} = \frac{1}{2\pi} \frac{|N(\omega)| \lambda}{|S(\omega)| \Delta x}$$

where  $\lambda$  is the wavelength and  $\Delta x$  is the distance over which the phase difference is measured [Aki and Richards, 1980]. Here  $S(\omega)$  and  $N(\omega)$  are the Fourier amplitudes of the signal and noise measured over the same

length of time. Phase velocity is measured more accurately for larger signal to noise ratio or for longer ranges. Lower-frequency waves are of larger wavelength, so higher signal to noise is required to measure phase velocity to comparable accuracy for a fixed range between source and receiver.

Figure 7 shows estimates of the signal amplitude  $S$  and noise  $N$  in one-third octave bands. The signal to noise ratio for Rayleigh waves from an earthquake typically falls rapidly with increasing wave period for both pressure and acceleration measurements. For periods shorter than 35 s, the SNR depends on noise amplitudes in the noise notch, which are limited by instrument noise for pressure sensors. At longer periods in the Pacific, the signal to noise ratios for surface waves for both vertical acceleration and pressure measurements depend on the amplitude of the infragravity wave spectrum, and the SNR for pressure is always lower.

The highest-resolution surface wave experiments use pairs of receivers separated by less than a wavelength. If we assume  $\lambda/\Delta x = 1$ , a signal to noise ratio of 24 dB (16 in amplitude) is required to obtain an accuracy of 1% in the phase velocity measurements. At 20-s period, the modeling suggests this SNR is obtained from earthquakes larger than about  $5.3 M_s$  for pressure measurements and about  $4.8 M_s$  for vertical acceleration (for observations from a low-noise, long-period instrument).

The long-period spectrum from the OSN-1 site (Figure 1) is thought to be typical of most ocean sites, with the exception of the North Atlantic in summer and the Arctic in winter, when much quieter infragravity wave conditions may prevail. In the Pacific, spectral levels in pressure of  $10^4 \text{ Pa}^2/\text{Hz}$  are associated with vertical acceleration spectral levels of about  $5 \times 10^{-16} (\text{m/s}^2)^2/\text{Hz}$  in the band from 100- to 200-s period [Crawford *et al.*, 1991]. North Atlantic conditions are sometimes 20–30 dB lower in pressure [Webb *et al.*, 1991] consistent with the acceleration noise levels seen by Beauduin and Montagner [1996] during the summer (Figure 17).

Energetic infragravity waves in the Pacific preclude

useful measurements of Rayleigh waves with pressure gauges at long period from all but the largest earthquakes. A  $M_s = 8.0$  earthquake is required to obtain a SNR of 24 dB for pressure measurements to periods as long as 200 s, while a  $M_s = 6.7$  earthquake provides a similar SNR for quiet North Atlantic conditions (dashed lines, Figure 7). In contrast, for acceleration measurements at 200-s period, a SNR of 24 dB can be obtained from  $M_s = 7.0$  earthquakes in the Pacific and from  $M_s = 5.5$  earthquakes for sites with quiet North Atlantic conditions. Actual SNRs for earthquakes will vary tremendously from these estimates. Records of Rayleigh waves from short-period inertial sensors are limited by instrument noise, but the lower-noise instruments can provide useful observations to periods as long as 100 s from the very largest earthquakes and for periods of 20–40 s from most earthquakes greater than  $M_s = 6.0$ . With better amplifiers, 1-Hz sensors could provide useful observations of Rayleigh waves to even longer period, although with poorer SNR than from true long-period instruments.

The band from 0.3 mHz to 20 mHz includes the eigenfrequencies of the first 2000 normal modes (free oscillations) of the Earth. On the seafloor the noise level in this band is set by the infragravity waves or by flow noise in regions of strong currents. Only since the installation of the IDA network of LaCoste-Romberg gravimeters in the 1970s has routine detection of normal modes been possible at continental sites [Agnew *et al.*, 1986]. This network also provided the first systematic measurements of vertical seismic noise at very low frequencies worldwide [Agnew *et al.*, 1986]. The vertical acceleration noise spectra at quiet continental sites are below  $10^{-18}$  (m/s<sup>2</sup>)<sup>2</sup>/Hz in the band from 0.2 to 20 mHz. The variance in 1-mHz bands is therefore about  $3 \times 10^{-11}$  m/s<sup>2</sup>. Initial mode amplitudes from very large earthquakes ( $M_s = 8$ ) may be larger than  $10^{-9}$  m/s<sup>2</sup> [Aki and Richards, 1980]. The decay of most normal modes spreads energy over a bandwidth of about 0.25 mHz, so for large earthquakes the narrow-mode peaks stand 20–30 dB above the noise. The vertical noise level on the Pacific seafloor is typically more than 20 dB higher than that at quiet continental sites in the normal mode band (Figures 1 and 7), so obtaining useful measurements on the seafloor of normal mode eigenfrequencies from even the largest earthquakes will be difficult. The integrated rms noise in a 0.25-mHz band near 10 mHz will exceed  $3 \times 10^{-10}$  m/s<sup>2</sup>.

Acceleration spectra from the central North Atlantic [Beauduin and Montagner, 1996] show noise levels comparable to those at good continental sites and suggest that useful normal mode measurements could be attained in this ocean basin under favorable weather conditions. Measurements obtained with an electrochemical broadband seismometer near the Reykjanes Ridge also showed very low noise levels, but much higher levels were found near the Canary Islands [Dozorov and Soloviev, 1991].

The Arctic Ocean in winter may also provide quiet sites for long-period measurements, since the ice cap prevents the propagation of ocean waves [Webb and Schultz, 1992]. Infragravity wave energy is expected to be high in the Indian Ocean and in the southern Atlantic because of the energetic ocean wave climate in the Southern Ocean. This should preclude any useful normal mode measurements from the seafloor south of the equator. A possible exception might be sites under the ice shelf around Antarctica in winter, but no measurements have yet been made to confirm this hypothesis.

## 16. NOISE NOTCH

The noise notch, the band in the deep-sea pressure spectrum above the infragravity waves at 0.03 and below the microseisms at 0.1 Hz, is important to marine seismology because it provides a low-noise window for the detection of Rayleigh waves and long-period body waves (Figure 2). The single-frequency microseism peak near 0.07 Hz in the noise notch is a permanent feature of spectra from either the seafloor or from land, although the peak can be partly obscured in Pacific seafloor measurements, (but not in the Atlantic [e.g., Babcock *et al.*, 1994]) by the side of the main (double frequency) microseism peak at 0.2 Hz.

The origin of the single-frequency peak is loosely associated with direct transfer of ocean wave energy into elastic waves through nonlinear coupling of waves and bathymetry [Hasselmann, 1963]. Measurements from instruments in coastal regions show energy that tracks swell incident at the coast, but this energy decays quickly inland [Haubrich *et al.*, 1963; Haubrich and McCamy, 1969]. Single-frequency peaks studied at nearshore and island stations are larger in amplitude than those at seafloor sites. The peak on Taiwan is 20 dB larger than that at typical seafloor sites and is higher frequency because the low-frequency swell components are removed by the broad shelf around the island [Hedlin and Orcutt, 1989].

In the center of ocean basins or continents, the single-frequency peak is related to large storm waves on remote coastlines [Cessaro, 1994]. The universality of the single-frequency peak suggests global sources. For example, Oliver [1962] reported a prominent source of very low-frequency microseisms along the southwestern African coast. The single frequency peak at the OSN-1 site south of Hawaii was 5 dB more energetic than that at continental site PFO (Figure 1), but the peak seen in Atlantic seafloor measurements [Beauduin and Montagner, 1996] was nearly 20 dB smaller than that at station SSB in Saint Sauveur Badol, central France (on the vertical component).

Below the single-frequency peak, reported levels in the noise notch in pressure vary from  $10^{-2}$  Pa<sup>2</sup>/Hz to about 10 Pa<sup>2</sup>/Hz. The noise level appears to be determined by instrumental noise, except at a few sites on the

deep seafloor ocean where currents obviously affect noise levels [Webb, 1988]. DPG sensor noise can be explained by standard  $1/f$  noise mechanisms for voltage fluctuations in current-carrying resistors [e.g., Scofield *et al.*, 1985].

There is little understanding of either the temporal or geographical variability of vertical component noise levels in the noise notch at present. *Beauduin and Montanger* [1996] observed small variations in vertical noise levels in this band during a weeklong experiment. Low noise levels were periodically interrupted by energetic Rayleigh wave trains from moderate earthquakes. *Sutton and Barstow* [1990] suggest higher noise levels in the noise notch on the vertical component during the passage of a hurricane. The mechanism for this change in noise level is unknown, although noise from digitization of the original records with resulting spectral leakage is a possibility. Horizontal noise levels for seafloor sensors are invariably controlled by currents.

Every few days a major earthquake generates Rayleigh waves that raise the pressure spectral levels in the noise notch in the Arctic for intervals of up to an hour (Figure 22). The long decay time in the oceans appears to be associated with reverberation within the ocean at frequencies between 10 and 15 s. The resemblance of the spectral shape of the single-frequency peak to the spectrum of earthquake Rayleigh wave trains from large earthquakes led *Lahav et al.* [1986] to speculate that the single-frequency peak was just the long-lived reverberant Rayleigh waves from many small to moderate earthquakes. This suggestion is not consistent with the studies of microseisms from large land-based arrays such as the large-aperture seismic array (LASA) in Montana [e.g., *Capon*, 1969], which show strong biases in source location. The array data also show the energy in the single-frequency peak propagates primarily as fundamental mode Rayleigh waves [*Lacoss et al.*, 1969].

## 17. INFRAGRAVITY WAVES

The vertical acceleration noise spectrum on the seafloor near Hawaii has been observed to be 10 dB more energetic at 0.03 Hz (30 s), and 25 dB more energetic at 0.01 Hz (100 s) than noise levels at the nearby station Kipapa on the island of Hawaii (Figure 1). Elevated noise levels at long period are due to the deformation of the seafloor under low-frequency, freely propagating ocean waves. This noise source is important below 0.03 Hz on the deep (4–5 km) seafloor and extends to higher frequencies at shallower depths: 0.04 Hz at 700 m and 0.05 Hz at 200 m.

Most of the energy in the ocean wave spectrum is in wind-driven waves at frequencies less than 0.04 Hz. Ocean waves at lower frequency are called “infragravity” waves and are generated by nonlinear processes from the wind waves and swell [*Webb et al.*, 1991]. Freely propagating ocean waves are governed by the dispersion

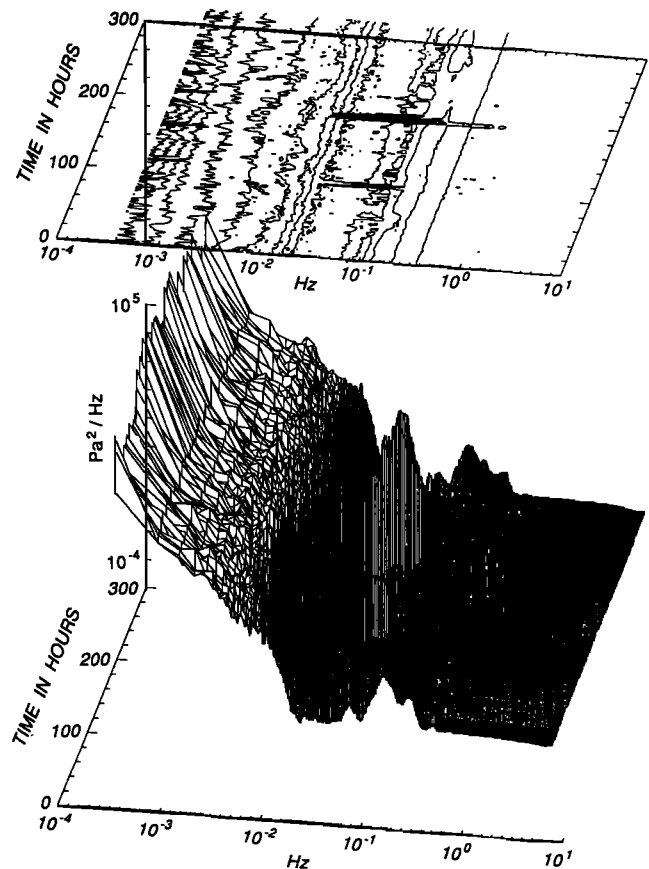


**Figure 22.** Series of spectra from the Arctic showing the occasional earthquake raising noise levels at long period above the very low background (reprinted with permission from *Webb and Schultz* [1992]; copyright 1992 Acoustical Society of America)

relation:  $\omega^2 = gk \tanh(kh)$  where  $h$ ,  $\omega$ , and  $k$  are the water depth, frequency, and wavenumber, respectively. Waves travel at roughly constant phase velocity at low frequencies for which the wavelength is large compared with the water depth ( $kh \ll 1$ ):  $C_p \approx (gh)^{1/2}$ . Phase speeds for long waves increase from 45 m/s at shelf depths (200 m) to over 200 m/s in 4-km depth. A 100-s-period infragravity wave will have a wavelength of 1 km in 10 m of water, increasing to 4.5 km in 200-m depth and to 20 km in deep water. The pressure signal from all ocean waves is evanescent in the vertical, decaying away from the sea surface with an  $e$ -folding scale equal to the wavenumber [*Kinsman*, 1984]. Ocean waves produce no discernible pressure signal at normal wind wave and swell frequencies ( $>0.05$  Hz) at the deep seabed because  $kh \gg 1$ . The exponential dependence on wavenumber of the seafloor pressure signal leads to a sharp high-frequency cutoff to the infragravity wave pressure spectrum at the seafloor (Figures 2 and 3).

Infragravity wave amplitudes in deep water are small, less than 1 cm in wave height in the band from 0.002 to 0.03 Hz. Despite the small amplitude, the wave signal dominates the seismic noise background on pressure

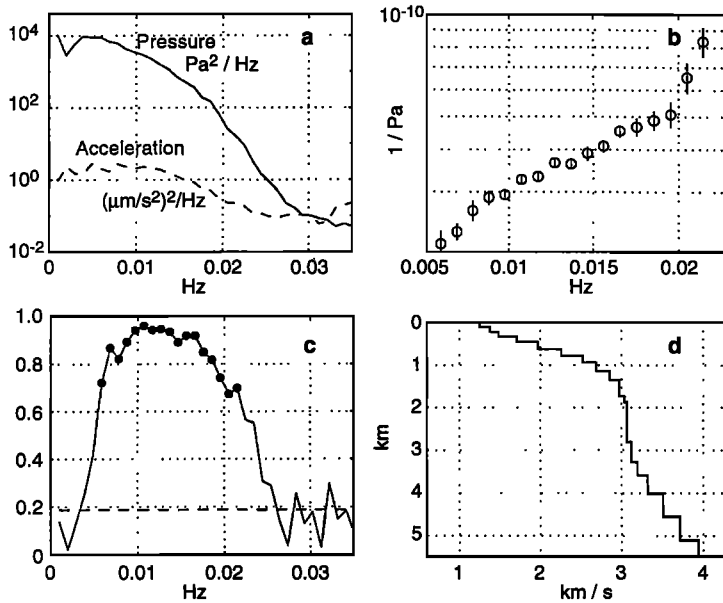


**Figure 23.** (a) Pressure and vertical acceleration spectra in the infragravity wave band. (b) Normalized compliance function between acceleration and pressure. (c) coherence between acceleration and pressure. (d) model of shear velocity below the site based on data in Figure 23b.

gauges directly, and the acceleration spectrum either at the seafloor or in a borehole is controlled by displacement of the seabed under the loading of these waves. Measurements of vertical acceleration at the deep seabed are strongly coherent with the pressure signal at frequencies below 0.03 Hz because of the deformation signal (Figure 23).

Measurements of the transfer function between pressure and the displacement under the loading of the ocean waves can be used to determine the elastic parameters below a site in a similar manner to using ocean load tides to investigate structure near continental boundaries [Beaumont and Lambert, 1972]. Yamamoto and Torii [1986] and Yamamoto *et al.* [1989] have used measurements of the deformation under short-period waves at several sites on the shallow shelf to determine the shear modulus below the seabed to depths of a few tens of meters. Low-frequency infragravity waves in deep water can also be used to probe the Earth, although displacement amplitudes are many orders of magnitude smaller than the displacements seen in shallow water, so the measurements are much more difficult. The larger wavelengths associated with deepwater infragravity waves allows the method to be used to probe more deeply. Recent work has investigated elastic structure through the entire oceanic crust [Crawford *et al.*, 1991, 1994]. Below 3 mHz it is important to consider effects of the infragravity waves other than the direct loading, including the gravitational attraction of the water mass in the wave and the changing value of gravity with vertical displacement of the seismometer.

Measurements of the transfer function between pressure and vertical acceleration at a ridge crest site are inverted using linear inverse theory to derive an Earth model (Figure 23). The shorter-period infragravity waves deform only the shallower parts of the crust, while the deformation under longer (lower frequency) waves

reaches through the entire crust. Measurements of the deformation signal are most useful for detecting regions of low shear modulus, which show up as peaks in the pressure to acceleration transfer function. Such regions may be associated with partial melt. Elastic parameters in regions with high shear modulus are poorly constrained by the technique, as the effects of regions of low shear modulus dominate. The technique is now being used to study 3-D structures such as ridge crest magma bodies and analyzed using finite difference techniques.

The seafloor acceleration spectrum can be predicted from the seafloor pressure spectrum using an Earth model for the site. For the purposes of predicting seafloor noise levels from infragravity wave spectra, the possible variations in acceleration amplitude associated with different models for seafloor structure are small. The acceleration spectrum near 0.02 Hz at hard rock sites should be 10–15 dB lower than at sedimented sites [Crawford *et al.*, 1991]. The difference in acceleration amplitudes between hard rock and mud becomes smaller at lower frequencies as deeper structure becomes more important.

Infragravity waves drive horizontal motions directly that are comparable in amplitude to the vertical motions (Figure 24). In contrast to ground motion on land due to atmospheric pressure noise, the effect on the horizontal components of tilting due to the deformation signal is small because the infragravity wave wavelengths are large. The vertical acceleration is always  $180^\circ$  out of phase with the pressure signal, as the waves act to push the bottom down, but the horizontal acceleration transfer function (Figure 24) can change sign with frequency for some Earth models [Crawford *et al.*, 1991]. Horizontal displacements induced by infragravity waves have not been observed at deep seafloor sites because of measurement difficulties; the flow noise is usually orders of magnitude larger. Presumably, with installation of the

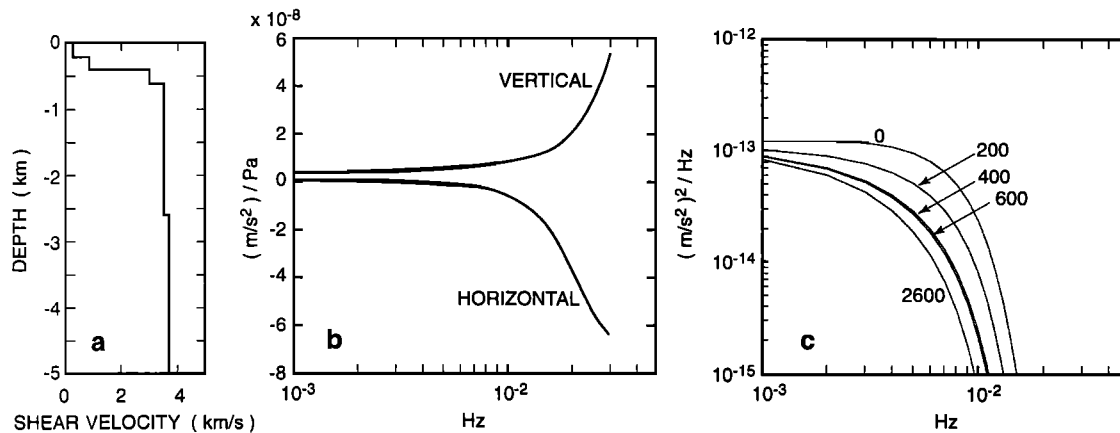


**Figure 24.** (a) shear velocity in a model of sedimented ocean crust. (b) Transfer functions between seafloor pressure and seafloor acceleration due to infragravity waves. (c) Predicted acceleration spectrum due to infragravity waves at five depths below the seafloor.

sensors below the seafloor to remove flow noise, infragravity waves will control long-period seismic noise levels for both horizontal and vertical components as well as strain (pressure).

The infragravity wave signal remains significant to depths of many kilometers below the seabed depending on the frequency, and the elastic parameters as a function of depth. Figure 24 shows predictions for the vertical acceleration due to infragravity waves at five depths in a model consisting of 400 m of sediment over basalt. The vertical deformation at 100-s period is 20 dB lower at the rock-sediment interface than at the seafloor and is 10 dB lower at 200-s period.

## 18. ORIGIN AND CLIMATOLOGY OF INFRAGRAVITY WAVES

The low-frequency noise spectrum at the seafloor in both pressure and vertical acceleration will usually be controlled by the amplitude of the infragravity wave spectrum. There are at least two mechanisms that drive infragravity waves. The existence of two different generating mechanisms is evident in the inflection in the slope of deep-sea pressure spectra near 0.002 Hz. At frequencies lower than 2 mHz, the pressure spectrum varies

inversely with the square of frequency [Filloux, 1980, 1983; Chave *et al.*, 1992]. This relation holds for frequencies from the tidal band to 0.002 Hz. Infragravity waves in this band may be driven directly by atmospheric pressure fluctuations in shallow water (rather like seiches in a lake), but there are no observations to support this hypothesis. The pressure spectrum below 0.002 Hz is remarkably constant in amplitude, with no apparent seasonal cycle. Pressure spectra measured at the seafloor in the Atlantic, Pacific, and Arctic Oceans are similar below 2 mHz (Figure 2).

At higher frequencies ( $>0.002$  Hz), infragravity wave amplitudes in the North Atlantic can be directly connected to the short-period ocean wave energy around the Atlantic basin [Webb *et al.*, 1991]. Infragravity wave energies varied by more than 25 dB during an 80-day interval in late fall 1985 (Figure 25). It is this relationship between short- and long-period waves that makes it possible to predict infragravity wave energies, and hence long-period seismic noise, at any site within the oceans.

Energy is coupled from short-period waves into long-period waves as ocean waves steepen and become very nonlinear in the shallow water of the surf zone. Two mechanisms have been proposed for coupling short-period wave energy into long-period energy at a beach. Groups of short-period waves are associated with long-wavelength bound waves that are locked to the wave groups so that the sea level is depressed under the largest waves [Longuet-Higgins and Stewart, 1964]. Treverrow *et al.* [1989] present measurements that show a large spectral peak in the infragravity wave band that appears to be caused by bound waves tied to a 15-s swell. The short waves break and dissipate at the shore, leaving the longwave components as low-frequency changes in sea level that couple into outgoing waves [Gallagher, 1971]. A second mechanism for low-frequency wave generation depends on a coupling between the distance offshore of the wave breakpoint and wave setup [Symonds *et al.*, 1982].

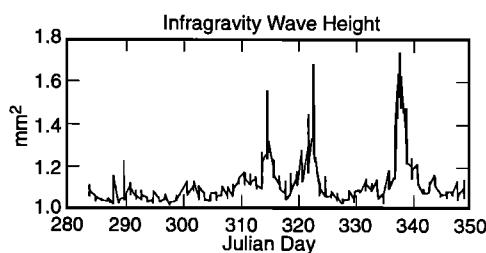


**Figure 25.** Variation of infragravity wave energy in the North Atlantic during an 80-day interval inferred from the amplitude of pressure fluctuations in a band near 0.007 Hz.

Most long-period energy is trapped within 1 km of the coastline, where it is called “surf beat.” Energy is coupled into distinct modes of a waveguide formed by the sloping bathymetry near the coast, which refracts long-period wave energy into the coast as ocean waves travel faster in deeper water [Munk *et al.*, 1964; Huntley *et al.*, 1981; Oltman-Shay and Guza, 1987]. The loading associated with coastally trapped infragravity waves produces local ground deformations that raise noise levels at long-period stations near the coast, including LJC (LaJolla, Ca) and RAR (Rarotonga). At these stations there are large variations in spectral amplitude at frequencies above 3 mHz depending on local wave conditions [Agnew and Berger, 1978], but because infragravity wave wavelengths in shallow water are short (<1 km) the deformation signal decays rapidly inland. Long-period seismic measurements on the seabed near the coast can be 30 dB noisier than deep seafloor observations. The ground deformation signal caused by the coastally trapped waves is very large even in water depths reaching 1000 m (Figure 3).

A small fraction of the low-frequency wave energy leaks off the shelf into deep water, where it becomes freely propagating ocean waves [Okiihiro *et al.*, 1991; Webb *et al.*, 1991]. In deep water, most of the wave energy is in “free” waves from distant sources, but there is a small component in bound waves tied to the short-period wave groups overhead. The pressure signal from bound waves is negligible at the deep seafloor except at very low frequency because the wavelengths are otherwise short compared with the water depth [Webb *et al.*, 1991]. In shallow water, bound waves become a more significant component of the pressure signal seen at the seabed [Okiihiro *et al.*, 1992]. The fraction of energy in bound waves on the continental shelf varies from 0.1 to 30% [Herbers *et al.*, 1994, 1995].

The phase speed of an infragravity wave increases from less than 10 m/s to over 220 m/s in deep water with a corresponding increase in wavelength. In deep water, infragravity waves travel almost without attenuation [Lighthill, 1979], so that waves travel across the ocean basins essentially unaltered, following approximately great circle paths. Bathymetry provides some gentle steering in the same manner as tsunamis [e.g., Guiborg *et al.*, 1997]. On reaching the opposite continental shelf, waves reflect with a reflection coefficient that is poorly known. Tsunamis are observed to decay with an  $e$ -folding time constant roughly proportional to the travel time across the basin, suggesting a loss of about  $1/e$  during reflection at a coastline [VanDorn, 1984, 1987]. Larger damping on the shelf is likely to establish a smaller reflection coefficient for the shorter-period waves of interest here.

North Atlantic sites have been found to be more variable and between 10 and 30 dB quieter than sites in the Pacific [e.g., Webb *et al.*, 1991; Babcock *et al.*, 1994]. The timescale of variability for a North Atlantic record (Figure 25) is set by the meteorology, with energetic

intervals identified with specific storms in the North Atlantic. A less energetic long-period pressure spectrum is expected to be associated with a quieter seafloor vertical acceleration spectrum. The vertical acceleration spectra measured in the infragravity wave band using a seafloor sensor and a sensor in a borehole near the Mid-Atlantic Ridge at 30°N [Beauduin and Montanger, 1996] were found to be 30 dB quieter than measurements from the OSN-1 site in North Pacific (Figures 1 and 17). The North Atlantic data can be reconciled with the Pacific observations if the infragravity wave energy during the period of observations was close to the lowest levels inferred from the 80-day pressure record of Webb *et al.* [1991] from the fall in the North Atlantic (Figure 25). The Atlantic acceleration measurements were obtained in midsummer, when the wave climate is the quietest in the Atlantic (Figure 14).

The convoluted shape of the North Atlantic basin shields the central basin from infragravity waves from the Arctic and Antarctic regions, resulting in much greater variability and lower longwave energy than in the Pacific [Webb *et al.*, 1991]. A wider average shelf may also lead to larger attenuation and a less energetic infragravity wave climate in the North Atlantic. In the Pacific, pressure spectra in the infragravity wave band are invariably between  $5 \times 10^3$  and  $5 \times 10^4$  Pa<sup>2</sup>/Hz. Storms in the northern hemisphere in winter and in the southern hemisphere in the summer, as well as typhoons in both seasons, act to maintain an energetic infragravity wave climate throughout the Pacific. Luther *et al.* [1990] and Webb *et al.* [1991] located a prominent seasonally varying source region near Vancouver Island using data from arrays of seafloor pressure sensors in the Pacific. Infragravity wave levels may be lower in some of the nearly enclosed seas of the Pacific (such as the Sea of Japan or China Seas) and in the eastern Indian Ocean because of the shielding by backarc island chains.

One set of measurements from the South Atlantic at 35°S demonstrates that the South Atlantic can be as noisy in the infragravity wave band as the North Pacific (J. Orcutt, personal communication, 1996). The South Atlantic is illuminated by the great waves of the circumpolar Antarctic ocean, while ray paths to the North Atlantic are obstructed by the coastlines of Africa and South America. It is likely that the Indian Ocean basin will also be noisy at long periods because it too is exposed to the great storm waves of the Southern Ocean. The Indian Ocean also experiences monsoons and typhoons during part of the year.

The Arctic seafloor was found to be very quiet in the infragravity band during the winter because the ice cover prevents the propagation of short-period ocean waves entirely [Webb and Schultz, 1992], but damping at very long period due to the ice is relatively weak, and long-period waves driven by the wind have been observed on the ice [Hunkins, 1962]. A interesting possibility is that the ice-covered seas that surround Antarctica in winter could provide good long-period sites at the seafloor if a

method to deploy instruments beneath the ice can be established.

The deformation of the seafloor under infragravity waves establishes the noise floor for long-period seismic measurements on the seabed. The difference in noise levels at 100-s period between the worst site in the Pacific and the quietest observations from the North Atlantic is about 30 dB. The noisiest sites will be comparable to noisy island sites for long-period seismology, while the quietest data are similar to data from the best continental sites.

## 19. OCEAN FLOOR CURRENTS AND LONG-PERIOD NOISE

Horizontal component noise at instruments deployed on the seafloor appears to be controlled primarily by ocean floor currents even though most of the ocean floor is relatively quiescent (see section 11). Long-period horizontal component noise levels were 30–40 dB higher than vertical noise levels (Figure 17) and varied with the current (and phase of the tide) at a Pacific site [Sutton *et al.*, 1965]. A similar difference in noise levels between vertical and horizontal components was found at a North Atlantic site [Beauduin and Montagner, 1996].

Ocean currents perturb sensors by pushing directly on the sensor package and by deforming the seafloor under the package, both of which cause tilting of the sensor package [Webb, 1988]. These sources of noise can usually be avoided by burying the sensors to a few meters' depth into the sediment. Deeper burial (30–60 m) may be required to fully escape the deformation signal in a few regions with very strong currents ( $>0.3$  m/s). Seismometers measure accelerations that are a tiny fraction of the Earth's gravity. At a quiet continental site a seismometer may see vertical accelerations smaller than  $10^{-10}$  m/s<sup>2</sup> in a 0.01 Hz band near 100-s period. A fluctuating tilt of  $10^{-11}$  rad will produce a comparable signal on the horizontal components as the acceleration of gravity is rotated into the horizontal components. It is evident that the forces associated with even quite weak currents are sufficient to cause the tilts necessary to raise long-period horizontal noise levels for any seismometer on the seafloor [Duennebier and Sutton, 1995; Webb, 1988].

A large number of compliance measurements as well as the measurements in Figure 17 demonstrate that good long-period vertical component measurements can be obtained from instruments deployed directly on the seafloor. The current noise on the vertical component is usually more than 20 dB below the infragravity wave signal at frequencies near 0.01 Hz [e.g., Crawford *et al.*, 1991]. Low noise levels on the vertical component can be achieved only if the vertical component is closely aligned with the true vertical; otherwise, tilt noise is rotated into the vertical component, with the noise proportional to the sine of deviation from the true vertical. Vertical

alignment for most seismometer systems is often not much better than 1°. For example, the STS-2 specification for alignment of the vertical is only 0.6°, suggesting that about 1 part in 100 of the tilt noise (in amplitude) will be rotated into the vertical component. Tilt noise is also coupled into the vertical if the rotation of the sensor package lifts the seismometer vertically [Duennebier and Sutton, 1995], but this term is likely to be important only at higher frequencies, since the acceleration noise from this source is proportional to the second time derivative of the tilt signal, while the misalignment signal is directly proportional to tilt.

On the continents, seismic noise at low frequencies at quiet sites is driven by ground deformation under local pressure fluctuations within the atmospheric boundary layer [Sorrells, 1971; Sorrells and Goforth, 1973]. Noise levels increase with wind velocity. Vertical component acceleration spectra are roughly flat in the period band from 20 to 200 s. Horizontal acceleration spectra are “red,” with levels increasing rapidly with increasing period; are more variable; and range from 10 to 50 dB noisier than vertical section [Peterson, 1993]. It is usual practice even for a temporary site to dig the seismometer into the ground to provide better coupling and to get the sensor out of the direct effect of the wind. Trevorrow *et al.* [1989] and Duennebier *et al.* [1991] have demonstrated that much lower noise levels can also be obtained at sites under the ocean for high-current shelf sites by burying sensors at shallow depths into the sediments.

At land sites the deformation signal attenuates slowly with depth, so that it is advantageous to deploy long-period sensors into boreholes to depths of about 100 m. Although one of the most important reasons cited for installing long-period seismometers in boreholes below the ocean floor is the avoidance of noise due to bottom current [Purdy and Dziewonski, 1988], it is likely that shallow burial (2 m) will almost always be adequate to avoid this source of noise at marine sites. Only at some unusual locations will deep ocean currents produce turbulent boundary layers with pressure fluctuations comparable in magnitude to wind-driven pressure fluctuations [Webb, 1988]. Even at these sites, it will not be necessary to place the sensor as deep as 100 m.

An eddy in a boundary layer with a characteristic wavelength  $X$  advects by a sensor at a speed near the free stream current velocity  $U$ , producing a characteristic period for the disturbance of  $T \approx X/U$ . In the atmospheric boundary layer the typical wind velocity may be 5–20 m/s, so that a 10-s-period disturbance is associated with wavelengths of 50–200 m. The deformation signal decays with depth following an  $e$ -folding scale set by the wavenumber and is reduced by 55 dB at a depth below the ground equal to one eddy diameter. At very long period ( $>200$  s), the wavelengths become so large that there is little difference in SNR for sensors in boreholes compared to surface vaults on competent ground. Below 0.4 mHz, seismic noise on land is strongly correlated with atmospheric pressure [Zum and Widmer,

1995]. At short periods, borehole noise levels may ultimately be determined by atmospheric infrasound, which does not attenuate with depth [Sorrells and Douze, 1974]. Atmospheric pressure fluctuations produce negligible signals at the deep seabed at frequencies of interest to seismologists.

At sites in a few unusual regions of the deep sea with energetic currents (30 cm/s) the eddy scale may become large enough to warrant burying sensors tens of meters below the seafloor. Observations from a strong current region on the Nova Scotia Rise showed pressure fluctuations in the noise notch (Figure 16) which varied as the fourth power of the current velocity [Webb, 1988]. The pressure spectrum of the flow related noise was found to vary in frequency as  $f^{-1.5}$  [Webb, 1988] in close agreement with observations of pressure fluctuations in the atmospheric (wind driven) boundary layer under stably stratified conditions [Elliot, 1972]. The amplitude of the pressure fluctuations in this ocean floor boundary layer were comparable to those seen in typical atmospheric boundary layers. The rms pressure fluctuations depend on the density  $\rho$  and flow velocity  $U$  as  $P_{\text{rms}} \approx 0.003\rho U^2$ . A wind velocity of 6 m/s or a water current velocity of 0.3 m/s both produce a rms pressure signal of about 0.3 Pa.

The scale of the eddies in a 0.3-m/s current reaches 60 m at periods of 200 s, suggesting that at sites under strong currents it might be useful to bury sensors as deep as 60 m. For more typical ocean floor sites where current velocities are less than 5 cm/s, the deformation noise at the surface will be nearly 30 dB smaller than the levels seen on the Nova Scotia Rise site, and the noise at 100-s period will be reduced by another 20 dB by burial to a depth of 2 m. Shallow burial to a depth of 1–2 m will be usually be adequate to avoid current-related noise.

## 20. BOREHOLE AND SUBSURFACE INSTALLATIONS AT LONG PERIOD

Section 10 discussed the improvements in signal to noise ratio for short-period measurements that can be obtained by installing instruments into deep boreholes in the seafloor. This section discusses the potential advantages to deep borehole installations for frequencies below the microseism peak. There are (at least) four important noise sources at periods longer than 10 s that affect detection of seismic phases. The primary frequency microseism peak from 0.06 to 0.1 Hz determines the vertical component noise level in the band from 10- to 20-s period. This energy propagates as fundamental mode Rayleigh waves, and no improvement in SNR is expected in this band unless the the seismometer is installed at very great depth (>10 km).

Currents control horizontal component noise at frequencies below 0.1 Hz at sites on the seafloor. Except at sites with very energetic currents, burial to a depth of 1–2 m should be sufficient to reduce flow-induced noise to negligible levels.

Biological noise is not discussed in this paper, but it can be a problem at all frequencies, as sea life bumps into sensitive seismometers. Shallow burial should put the seismometers out of reach of animals.

Infragravity waves provide the strongest incentive to consider deep borehole installations for long-period sensors, although the achievable improvement in SNR is small. Infragravity waves are the dominant noise source on the vertical component at periods longer than 30 s in deep water at sites in the North Pacific. At 400 m below the seafloor, the infragravity wave spectrum is reduced from seafloor values by about 10 dB at a period of 200 s and 10 dB at 100 s for the model shown in Figure 24. The smaller infragravity wave deformation signal at depth is due to a combination of a larger rigidity for rock compared to sediments and the evanescent decay of the signal with depth. Reducing the noise level in the band below 100 s will provide better records of surface waves. The improvement in SNR in the normal mode band (<2 mHz) is too small to make much of a difference in the usefulness of the typical noisy seafloor station for this purpose.

The need to improve the SNR for short period teleseismic phases provides the most compelling reason for installation of seismometers in deep boreholes into the seabed. The depth of burial is important because it greatly affects the cost of an installation. A deep borehole into rock can be drilled only using the Ocean Drilling Program (ODP) ship, which costs about \$60,000 per day to operate and is heavily subscribed for other work. Duennebier *et al.* [1991], Yamamoto *et al.* [1989] and L. D. Bibee (personal communication, 1996) have developed systems for placing seismometers at shallow depths in the sediments of the seafloor. The first system uses a remote-operated vehicle (ROV) and a jet of water to drive the sensors a short distance into the mud, and the second uses the ROV to place a caisson into which the sensors are installed. In the Bibee system a short-period seismometer is equipped with a drill that pulls the sensor package into the mud to a depth of as much as 10 m. The short-period sensor is decoupled from the recording package and abandoned in the mud to recover the instrument. It is conceivable that a system could be designed that would place a broadband sensor as much as a few tens of meters into mud using water jets, a gravity system (a heavy weight) or some other system, but nothing exists now. Such a system would be cheaper to operate than the drilling ship and more readily available.

There have been two previous experiments with long-period instruments in boreholes in which noise levels were compared with noise levels on the seafloor. A deployment of a Guralp CMG-3 three-component seismometer in ODP Hole 395 in the Sea of Japan is described by Suyehiro *et al.* [1995]. Unfortunately, the system gain was too low at long periods to provide much information about long-period noise in deep-sea boreholes.

*Beauduin and Montagner* [1996] and *Montagner et al.*

[1994] describe an experiment in the North Atlantic [Romanowicz *et al.*, 1984]. The instruments were installed using the submersible *Nautilé*. One instrument was placed into ODP Hole 396A, and the other was placed into an old reentry cone left on the seafloor during previous drilling. The vertical component noise levels of the two instruments were comparable in the microseism band (0.1–0.25 Hz). The seafloor instrument was 10 dB quieter than the borehole instrument at longer periods and noisier at shorter periods (Figure 17). Noise at both seafloor instruments was higher than the continental site SSB in central France at frequencies above the microseism peak. The vertical component long-period noise on the seafloor instrument was comparable to the noise level at station SSB. The horizontal components at the seafloor were 5–10 dB noisier than those at the land site below 0.05 Hz but were quieter between 0.05–0.3 Hz. The long-period noise level on the borehole instrument fell slightly during the 3 days of operation. The authors believe that the borehole instrument was disturbed by flow in the borehole, and they suggest that noise levels might have reached or surpassed the noise levels on the seafloor instruments after a longer interval. The horizontal components of the borehole instrument were very noisy, and the authors believe that the sensors were not working correctly. During future deployments of broadband instruments, either the boreholes should be filled with sand or the sensors should be grouted into the borehole with cement to avoid noise from flow in the borehole. Noise coupled into the borehole by motions of the massive reentry cone at the top of the borehole must also be considered a possible source of seismic noise in ocean floor boreholes.

## 21. CONCLUSIONS

The ocean floor is noisier than good continental sites for seismic measurements because ocean waves at the sea surface are an important and local source of noise. Microseisms from ocean waves are the largest noise source for both continental and oceanic stations, but the microseism peak is more energetic and broader at seafloor stations. This has important consequences for the detection of short-period body wave phases from teleseismic earthquakes. The vertical acceleration spectrum near 1 Hz can be 60 dB noisier at the seafloor than at continental sites. At most seafloor sites, short-period *P* waves from distant ( $>30^\circ$ ) earthquakes will be detectable only from the very largest earthquakes because of high noise levels and because the more easily detected high-frequency components are removed by attenuation.

Noise levels in the microseism peak at 1 Hz are determined by the ocean wave spectrum at 0.5 Hz in an area local to the site. Moderate breezes (5 m/s) are sufficient to raise the ocean wave spectrum to saturation levels at frequencies near 0.5 Hz so that only regions with nearly calm winds can be expected to experience

low seismic noise at 1 Hz. The equatorial regions of the eastern Atlantic, eastern Pacific, and Indian Oceans, and the central North Atlantic in summer are characterized by light winds more than 60% of the time. These regions are likely to provide low seafloor noise levels near 1 Hz and so provide good signal to noise ratios for short-period arrivals from teleseismic earthquakes of moderate amplitude ( $m_b > 5.5$ ). Outside of these regions, 1-Hz noise levels will be high, limiting the detection of short-period, teleseismic body waves to very large earthquakes ( $m_b > 7.5$ ).

Long-period noise levels are controlled by ocean currents and by long-period ocean waves called infragravity waves. Vertical component and pressure noise levels between 0.03 and 0.1 Hz will be moderate at most seafloor sites so that long-period body wave arrivals are observable from teleseismic earthquakes with magnitudes from  $M_s > 5.5$  at  $40^\circ$  range to  $M_s > 5.9$  at  $100^\circ$  range. However, observations are complicated by water column reverberations hidden by the low-pass filtering required to see the long-period arrivals below the microseism peak. Timing errors due to interference from reverberations can exceed 1 s and depend on the water depth and pass band of the filters used in the analysis. Vertical acceleration measurements are less affected by water column reverberations than pressure measurements and therefore provide more accurate rate determinations of long-period arrivals.

Long-period horizontal noise levels for sensors on the seafloor are much higher than vertical noise levels, and appear to be controlled by ocean floor currents. The sensors respond to very small amplitude tilting of the sensor package as the acceleration of gravity is rotated into the horizontal components. Noise levels vary by 30 dB or more between sites and with time, and increase rapidly with period. Observations show that during quiet intervals it is possible to detect long-period body waves with horizontal sensors in the period band from 10 to 20 s from large, teleseismic earthquakes ( $M_w > 6$ ). During noisy intervals, or at noisy sites, detection thresholds for long-period body waves on the horizontal components can be effectively 3 magnitudes higher and thus useless for long-period observations.

The vertical acceleration and pressure noise levels at periods longer than 30 s are controlled by the infragravity wave spectrum. The infragravity wave spectrum in the Pacific basin is always energetic because storm waves are always striking some part of the coastline. The long wave climates in the Indian and South Atlantic Oceans are probably also invariably energetic because these basins are exposed to the stormy Southern Ocean. The pressure spectrum is 50–60 dB noisier at periods near 100 s than between 10 and 30 s because of infragravity waves. The deformation of the seafloor under the loading of these waves raises vertical acceleration noise levels at periods near 100 s by 20–30 dB, so that useful surface wave data to periods as long as 200 s can be obtained from  $M_s = 6.6$  earthquakes using vertical component

seismometers. If pressure sensors are used, the threshold is increased to  $M_s = 8.0$  earthquakes.

The North Atlantic infragravity wave climate is considerably quieter and more variable. During quiet intervals, long-period vertical component noise levels may be as low as those at good continental sites, and earthquakes as small as  $5.5 M_s$  may provide good Rayleigh wave records to periods as long as 200 s. Vertical component noise levels may be low enough to provide useful measurements of normal mode eigenfrequencies. Pressure measurements will be useful to 200-s period from earthquakes as small as  $6.7 M_s$ . Noise levels will be much higher during the winter when the wave climate is more energetic. The Arctic and Antarctic regions may experience low long-period noise levels during winter, when the ice caps prevent the propagation of ocean waves in these regions.

The fidelity of short-period observations using ocean bottom seismometers is limited by the sensor coupling to a sedimented or rubble-strewn seafloor. Installation of the sensors below the seafloor, either by jetting the sensors into the mud or by installation in boreholes, will improve coupling. Burying the sensors to a few meters' depth is expected to improve long-period noise levels of horizontal component seismometers by 30 dB or more by shielding the sensors from tilting due to ocean floor currents.

Deep-sea boreholes can be used to place seismometers a few hundred meters below the seafloor. Placing sensors 100 m below the seafloor can improve the signal to noise ratio at 1 Hz by 5–10 dB for vertical component sensors and by 15 dB for horizontal component sensors compared with sensors on the seafloor. At 5 Hz the SNR for the sensors in the borehole can be 20 dB better than for sensors on the seafloor. Little additional improvement in signal to noise for short-period signals is expected by installation at depths greater than 100 m.

Long-period signal to noise ratios improve only slightly with depth of burial once the sensors are placed below the effects of currents, since the low-frequency infragravity wave deformation signal decays slowly with depth. Long-period noise levels from broadband seismometers installed in seafloor boreholes to date have been a disappointment, probably because of flow in the borehole driven by the hydrothermal gradient.

Many of the questions remaining about deep-sea installation of seismometers should be answered by the OSN-1 experiments to be conducted in 1998 [Orcutt, 1996]. Ocean bottom seismometers will be deployed nearby to broadband sensors installed into a deep seafloor borehole. Sensors will also be buried at shallow depths below the seafloor next to the borehole. These experiments should solidify our understanding of the depth dependence of seafloor noise.

Geographical and temporal variations in vertical component seafloor noise are probably larger than any possible improvement in SNR that can be obtained by better installation techniques. Choosing better sites may offer bigger gains in SNR than drilling deeper boreholes.

Noise issues should be included in considerations of the siting of temporary arrays of seismometers.

It seems likely that permanent ocean floor seismic stations will become a component of the global seismic network. There are still many engineering problems to be overcome, not the least of which is the problem of how to get the data back to land. This paper was written to remind seismologists that the seafloor is different. It is not possible to conduct the same kinds of experiments on the seafloor that can be done on land, and there are many regions of the world where adding seafloor stations may not provide any benefit because of noisy seafloor conditions.

## APPENDIX: THE AMPLITUDE OF BODY WAVE PHASES AT TELESEISMIC DISTANCES

The amplitude of a teleseismic body wave phase depends on the details of the earthquake source, the instrument location and ray path, and the geology at the receiver. The practical definition of a "detection limit" is the smallest magnitude at a particular range for which it is likely that the earthquake phase will be detected with sufficient signal to noise to be accurately picked. The detection limit here is assumed to be an average over all possible earthquake source parameters. In this paper it is based on a range of  $30^\circ$ .

The expert will recognize many omissions in the following discussion, but the models demonstrate some of the key differences between continental and oceanic sites: (1) the detection limit for teleseismic, short-period body waves is much higher at the typical seafloor site compared with the typical continental sites, while (2) the detection limit for local events is often lower at oceanic sites, and (3) the long-period body wave detection limit is similar at continental and ocean floor sites. The difference in detection limits is due to the noise climate rather than to different propagation characteristics under the ocean.

The detection limit in these models is defined in terms of the moment magnitude  $M_w$ , but the short-period body wave magnitude  $m_b$  and the surface wave magnitude  $M_s$  are more commonly measured. *Aki* [1976] suggests that the peak *P* wave amplitude must be about 20 times larger than the rms noise for the arrival time to be accurately measured and for the direction of first motion (polarity) to be certain. The model shown here examines the frequency dependence of the detection limit as though the signal was passed through a sequence of very narrow band filters.

The maximum attainable signal to noise ratio  $d$  for the detection of a transient signal with optimum filtering is

$$d^2 = \int \frac{|A(f)|^2}{P(f)} df \quad (\text{A1})$$

where  $P(f)$  is the power spectrum of the noise and

$A(f)$  is the amplitude spectrum of the signal [e.g., *McDonough and Whalen, 1995*].

To examine the signal to noise ratio for a body wave arrival as a function of frequency, consider a sequence of very narrow pass band filters of width  $\Delta f$ , centered around  $f_0$ . The noise power spectrum and signal amplitude spectrum are assumed to be approximately constant within this narrow band, so the previous equation simplifies, since the filtered signal is assumed to be zero outside  $|f - f_0| < \Delta f$ :

$$d(f_0) \approx \frac{|A(f_0)|\Delta f}{[P(f_0)\Delta f]^{1/2}} \quad (\text{A2})$$

The phase of the Fourier transform  $A(f)$  must be roughly constant across each narrow band for this equation to be a good approximation. This is true if the  $P$  wave pulse does not disperse significantly during propagation compared with the rise time of the filters. Scattering and other processes lengthen the shear wave body wave train significantly, making it difficult to estimate the peak horizontal accelerations needed for engineering calculations [e.g., *Ou and Herrmann, 1990*]. *Boatwright* [1982] has modeled the far-field acceleration spectrum assuming that the source function in acceleration consists of a series of discrete pulses associated with the fault rupture starting at a point and stopping at several locations on the periphery. These processes are ignored in modeling the detection threshold for the  $P$  wave.

One rule is to compare arrival amplitudes to noise in one-third octave bands with the expectation that this is the practical limit for narrowband filters [*Melton, 1976; Agnew et al., 1986*]. We take  $\Delta f = (2^{1/6} - 2^{-1/6})f_0$  and define  $S(f_0) = |A(f_0)|\Delta f$ ;  $N(f_0) = P(f_0)^{1/2}\Delta f$ , so that  $d = S/N$ . Here  $S$  and  $N$  are the amplitudes of the signal and noise as a function of the center frequency of the narrowband filter.

$S$  and  $N$  are calculated for both acceleration and pressure in Figure 7 for the  $P$  wave phase. Other compressional body wave phases should have similar amplitudes. Where  $S \gg N$  the signal should be visible in a narrowband filtered record. It may be useful or necessary to take a wider bandwidth for detection of an arrival. These curves overestimate  $S/N$  as the bandwidth is increased.

The compressional wave displacement spectrum  $U(f)$  is related to the moment rate spectrum  $M'(f)$  of an earthquake by

$$U(f) = M'(f) \frac{g(\Delta)R_{\theta\phi}C}{4\pi\rho\alpha^3R_E} \exp\left(-\frac{\pi ft^*}{2}\right) \quad (\text{A3})$$

where  $\rho = 2800 \text{ kg/m}^3$  and  $\alpha = 6700 \text{ m/s}$  are the density and  $P$  wave velocity at the source,  $R_E$  is the radius of the Earth,  $g(\Delta)$  represents the geometrical spreading,  $R_{\theta\phi}$  is the effective radiation pattern of the  $P$  wave train, and  $C$  describes the free surface effect or, in this paper, the transmission coefficient at the seafloor. For our purposes, we take  $C \approx 1.7$  to allow for a single reflection at

the seafloor. The exponential term with  $t^*$  models the attenuation between source and receiver [*Houston, 1990*]. The average  $R_{\theta\phi}$  is taken to be 0.52 following *Boore and Boatwright* [1984]. Attenuation acts to remove the higher-frequency components of the body wave phases. Typical continental values for  $t^*$  for  $P$  waves are near 1 s, so that teleseismic body wave arrivals contain energy in frequencies as high as a few hertz. Attenuation is higher in the upper mantle under the oceans and perhaps much higher under ridge crests. Models are shown with  $t^*$  ranging from 0 to 2 s.

The amplitude of the  $P$  wave body wave arrival as a function of frequency is estimated from (A3) and an earthquake source spectrum. The “ $\omega^2$ ” model for the moment rate spectrum finds wide application:

$$M'(\omega) = \frac{M_0\omega_c^2}{\omega_c^2 + \omega^2} \quad (\text{A4})$$

with a corner frequency given by [*Brune, 1970*]

$$\frac{\omega_c}{2\pi} = 5.7 \times 10^7 [M_0]^{-1/3} \quad (\text{A5})$$

The corner frequency relationship follows the parameters used by *Houston and Kanamori* [1986]. It is assumed that  $\Delta f$  is small compared to  $\omega_c/2\pi$ .

There has been much discussion over the validity of the various models for the displacement spectrum. The  $\omega^2$  model overestimates short-period spectral amplitudes for very large earthquakes [e.g., *Geller, 1976*]. An approximate relationship between moment  $M_0$  and surface wave magnitude  $M_s$  is

$$\log(M_0) = 1.5M_s + 16.1 \quad (\text{A6})$$

valid for  $M_s < 7.5$ . Both the surface magnitude  $M_s$  and the short body wave magnitude  $m_b$  scales saturate for very large earthquakes (large moment). This same equation is used to define the moment magnitude  $M_w$ :

$$M_w = 2/3(\log(M_0) - 16.1) \quad (\text{A7})$$

The short-period magnitude  $m_b$  is defined as

$$m_b = \log(A/T) + Q \quad (\text{A8})$$

where  $A$  is the maximum amplitude in the first five cycles of the waveform and  $T$  is the characteristic period, typically about 1 Hz for moderate earthquakes.  $Q$  is a complicated function of range. *Houston and Kanamori* [1986] report an alternative scale  $m_b$  that does not appear to saturate and that uses the largest amplitude seen at any time in the  $P$  wave train in the magnitude relation.

There is not a simple relationship between  $m_b$  and the displacement spectrum [e.g., *Geller, 1976*]. In the discussions in this paper,  $m_b$  and  $M_s$  are related using the Gutenberg-Richter relationship  $m_b = 6.75 + 0.63(M_s - 6.75)$  [*Aki, 1967*]. This formula overpredicts short-period magnitudes above  $M_s = 7.5$ .

The acceleration and pressure compressional wave rms amplitudes in one-third octave bands have been estimated for earthquakes with magnitudes  $M_w = 6, 7,$  and  $8$  for a distance of  $30^\circ$  (Figure 7). The models shown in Figure 7a are similar to the models of Agnew *et al.* [1986]. Increasing the distance to  $90^\circ$  would reduce the displacement amplitude by about one half [Kanamori and Stewart, 1976]. The rms noise in one-third octave bands observed at one seafloor site during a quiet and a noisy interval are compared with the predicted amplitudes for the earthquake arrival in Figure 7. We assume detection can be accomplished in any significant band for which  $S > 6N$ .  $N$  is equal to the noise variance in the band. A rule of thumb relates the peak to peak value in Gaussian noise to 6 times the rms. Thus with  $S = 6N$ , we have the amplitude of the signal roughly 18 times the rms noise, fitting Aki's [1976] rule as described earlier.

**ACKNOWLEDGMENTS.** I would like to thank Fred Duennebieer, John Hildebrand, Wayne Crawford, and an anonymous reviewer for reviews of the manuscript. This work was supported by the Office of Naval Research (N00014-96-1-0297).

Alan Chave was the Editor responsible for this paper. He thanks Fred Duennebieer and an anonymous referee for technical reviews, and Lisa Tauxe for the cross-disciplinary review.

## REFERENCES

- Adair, R. G., J. A. Orcutt, and T. H. Jordan, Analysis of ambient seismic noise recorded by downhole and ocean-bottom seismometers on deep sea drilling project leg 78B, *Initial Rep. Deep Sea Drill. Proj.*, 78, 767–780, 1984.
- Agnew, D. C., and J. Berger, Vertical seismic noise at very low frequencies, *J. Geophys. Res.*, 83, 5420–5424, 1978.
- Agnew, D. C., J. Berger, W. E. Farrell, J. F. Gilbert, G. Masters, and D. Miller, Project IDA: A decade in review, *Eos Trans. AGU*, 67(16), 203–212, 1986.
- Aki, K., Scaling law of seismic spectra, *J. Geophys. Res.*, 72(4), 1217–1231, 1967.
- Aki, K., Signal to noise ratio in seismic measurements, in *Volcanos and the Tectonosphere*, edited by H. Aoki and S. Iizuka, pp. 187–192, Tokai Univ. Press, Tokyo, 1976.
- Aki, K., and P. G. Richards, *Quantitative Seismology: Theory and Methods*, p. 298, W. H. Freeman, New York, 1980.
- Allen, S. E., and R. E. Thomson, Bottom-trapped subinertial motions over midocean ridges in a stratified rotating fluid, *J. Phys. Oceanogr.*, 23(3), 566–581, 1993.
- Babcock, J. M., B. A. Kirkendall, and J. A. Orcutt, Relationships between ocean bottom noise and the environment, *Bull. Seismol. Soc. Am.*, 84(6), 1991–2007, 1994.
- Beauduin, R., and J. P. Montagner, Time evolution of broadband seismic noise during the French pilot experiment OFM/SISOBS, *Geophys. Res. Lett.*, 23(21), 2995–2998, 1996.
- Beaumont, C., and A. Lambert, Crustal structure from surface load tilts, using a finite element model, *Geophys. J. R. Astron. Soc.*, 29, 203–226, 1972.
- Blackman, D. K., J. A. Orcutt, D. W. Forsyth, and J.-M. Kendall, Seismic anisotropy in the mantle beneath an oceanic spreading center, *Nature*, 366, 675–677, 1993.
- Blackman, D. K., J. A. Orcutt, and D. W. Forsyth, Teleseismic detection using ocean bottom seismometers at mid-ocean ridges, *Bull. Seismol. Soc. Am.*, 85(6), 1648–1664, 1995.
- Boatwright, J., A dynamic model for far-field acceleration, *Bull. Seismol. Soc. Am.*, 72(4), 1049–1068, 1982.
- Bolt, B. A., *Nuclear Explosions and Earthquakes: The Parted Veil*, W. H. Freeman, New York, 1976.
- Boore, D. M., and J. Boatwright, Average body-wave radiation coefficients, *Bull. Seismol. Soc. Am.*, 74(5), 1615–1621, 1984.
- Bradley, C. R., and R. A. Stephen, Modeling of seafloor wave propagation and acoustic scattering in 3-D heterogeneous media, *J. Acoust. Soc. Am.*, 100(1), 225–236, 1996.
- Bradley, C. R., R. A. Stephen, L. M. Dorman, and J. A. Orcutt, Very low frequency (0.2–10 Hz) seismoacoustic noise below the seafloor, *J. Geophys. Res.*, 102(B6), 11,703–11,718, 1997.
- Bratt, S. R., and S. C. Solomon, Compressional and shear wave structure of the East Pacific Rise at  $11^\circ 20' N$ ; Constraints from three-component ocean bottom seismometer data, *J. Geophys. Res.*, 89(B7), 6095–6110, 1984.
- Brink, K. H., Tidal and lower frequency currents above Fieberling Guyot, *J. Geophys. Res.*, 100(C6), 10,817–10,832, 1995.
- Brune, J. N., Tectonic stress and the spectra of seismic shear waves from earthquakes, *J. Geophys. Res.*, 75(26), 4997–5009, 1970.
- Butler, R., The Hawaii 2 observatory: A deep ocean geoscience facility reusing the Hawaii 2 telephone cable, in *Broadband Seismology in the Oceans: A Five Year Plan*, Joint Oceanogr. Inst., Washington, D. C., 1995.
- Butler, R., and F. K. Duennebieer, Teleseismic observations from OSS IV, *Initial Rep. Deep Sea Drill. Proj.*, 88, 147–153, 1989.
- Butler, R., C. S. McCreery, L. N. Frazer, and D. A. Walker, High frequency seismic attenuation of oceanic  $P$  and  $S$  waves in the western Pacific, *J. Geophys. Res.*, 92(B2), 1383–1396, 1987.
- Capon, J., Investigation of long period noise at the large aperture seismic array, *J. Geophys. Res.*, 74(12), 3182–3194, 1969.
- Carter, J. A., F. K. Duennebieer, and D. M. Hussong, A comparison between a downhole seismometer and a seismometer on the ocean floor, *Bull. Seismol. Soc. Am.*, 74(3), 763–772, 1984.
- Cessaro, R. K., Sources of primary and secondary microseisms, *Bull. Seismol. Soc. Am.*, 84(1), 142–148, 1994.
- Challenor, P. G., S. Foale, and D. J. Webb, Seasonal changes in the global wave climate measured by the Geosat altimeter, *Int. J. Remote Sens.*, 11(12), 2205–2213, 1990.
- Chave, A. D., D. S. Luther, and J. H. Filloux, The barotropic electromagnetic and pressure experiment, 1, Barotropic response to atmospheric forcing, *J. Geophys. Res.*, 97(C6), 9565–9593, 1992.
- Choy, G. L., and V. F. Cormier, Direct measurement of the mantle attenuation operator from broadband  $P$  and  $S$  waveforms, *J. Geophys. Res.*, 91(B7), 7326–7342, 1986.
- Claussen, J. P. J. Unger, and W. Leith, Performance estimates of a global network of open stations, *IRIS Newsl.*, 12(3), pp. 1–7, Inc. Res. Inst. for Seismol., Arlington, Va., 1993.
- Cox, C. S., S. C. Webb, and T. K. Deaton, A deep sea differential pressure gauge, *J. Atmos. Oceanic Technol.*, 1(3), 237–246, 1984.
- Crawford, W. C., S. C. Webb, and J. A. Hildebrand, Seafloor compliance observed by long period pressure and displacement measurements, *J. Geophys. Res.*, 96, 16,151–16,160, 1991.
- Crawford, W. C., S. C. Webb, and J. A. Hildebrand, The coaxial segment crustal magma source (abstract), *Eos Trans. AGU*, 75(44), Fall Meet. Suppl., 617, 1994.
- Der, Z. A., T. W. McElfresh, and A. O'Donnell, An investigation of the regional variations and frequency dependence of anelastic attenuation in the mantle under the United States

- in the 0.5–4.0 Hz band, *Geophys. J. R. Astron. Soc.*, 69, 67–100, 1982.
- Ding, X.-Y., and S. P. Grand, Upper mantle  $Q$  structure beneath the East Pacific Rise, *J. Geophys. Res.*, 98(B2), 1973–1985, 1993.
- Donelan, M. A., J. Hamilton, and W. H. Hiu, Directional spectra of wind generated waves, *Philos. Trans. R. Soc. London, Ser. A*, 315, 509–562, 1985.
- Dorman, L. D., A. E. Schreiner, L. D. Bibee, and J. A. Hildebrand, Deep water seafloor array observations of seismo-acoustic noise in the eastern Pacific and comparisons with wind and swell, in *Natural Physical Sources of Sound*, edited by B. R. Kerman, pp. 165–174, Kluwer Acad., Norwell, Mass., 1993.
- Dougherty, M. E., and R. A. Stephen, Seismic energy partitioning and scattering in laterally heterogeneous ocean crust, *Pure Appl. Geophys.*, 128, 195–229, 1991.
- Dozorov, T. A., and S. L. Soloviev, Spectra of ocean bottom noise in the 0.01–10 Hz range, *Geophys. J. Int.*, 106, 113–121, 1991.
- Duennebie, F. K., and G. H. Sutton, Fidelity of ocean bottom seismometers, *Mar. Geophys. Res.*, 17(6), 535–555, 1995.
- Duennebie, F. K., G. Blankington, and G. H. Sutton, Current generated noise recorded on ocean bottom seismometers, *Mar. Geophys. Res.*, 5, 109–115, 1981.
- Duennebie, F. K., C. S. McCreery, D. Harris, R. K. Cessaro, C. Fisher, and P. Anderson, OSS IV: Noise levels, signal-to-noise ratios, and sources, *Initial Rep. Deep Sea Drill. Proj.*, 88, 89–103, 1989.
- Duennebie, F. K., D. Harris, S. Poulos, and B. Hahn, A buried ocean bottom seismometer: Results from the ULF/VLF experiment (abstract), *Eos Trans. AGU*, 72(44), Fall Meet. Suppl., 303, 1991.
- Dziewonski, A. M., and D. L. Anderson, Preliminary reference Earth model, *Phys. Earth Planet. Inter.*, 25, 297–356, 1981.
- Dziewonski, A. M., et al., Background and objectives of the ocean seismic network, and leg 136 drilling results, *Proc. Ocean Drilling Program Initial Rep.*, 139, 3–98, 1992.
- Elliot, J. A., Microscale pressure fluctuations measured within the lower atmospheric boundary layer, *J. Fluid Mech.*, 53, 351–383, 1972.
- Ewing, M., and A. Vine, Deep-sea measurements without wires or cables, *Eos Trans. AGU*, 19(1), 248–251, 1938.
- Filloux, J. H., Pressure fluctuations on the open ocean floor over a broad frequency range: New program and early results, *J. Phys. Oceanogr.*, 10(10), 1959–1971, 1980.
- Filloux, J. H., Pressure fluctuations on the open ocean floor off the Gulf of California: Tides, earthquakes, tsunamis, *J. Phys. Oceanogr.*, 13(5), 783–796, 1983.
- Forysth, D. W., Teleseismic  $P$ -wave delays near the intersection of the Oceanographer fracture zone and the Mid-Atlantic Ridge (abstract), *Eos Trans. AGU*, 63(45), 1100, 1982.
- Forysth, D. W., Partial melting beneath a Mid-Atlantic ridge segment detected by teleseismic  $PKP$  arrivals, *Geophys. Res. Lett.*, 23(5), 463–466, 1996.
- Fox, C. G., W. E. Radford, R. P. Dziak, T. K. Lau, H. Matsumoto, and A. E. Schreiner, Acoustic detection of a seafloor spreading episode on the Juan de Fuca ridge using military hydrophone arrays, *Geophys. Res. Lett.*, 22(2), 131–134, 1995.
- Gallagher, B., Generation of surf beat by non-linear wave interactions, *J. Fluid Mech.*, 49, 1–20, 1971.
- Geller, R. J., Scaling relations and earthquake source parameters and magnitudes, *Bull. Seismol. Soc. Am.*, 66(5), 1501–1523, 1976.
- Gross, T. F., A. J. Williams III, and W. D. Grant, Long-term in-situ calculations of kinetic energy and Reynolds stress in a deep sea boundary layer, *J. Geophys. Res.*, 91(C7), 8461–8469, 1986.
- Gross, T. F., A. E. Isley, and C. R. Sherwood, Estimation of stress and bottom roughness during storms on the northern California shelf, *Cont. Shelf Res.*, 12(2/3), 389–413, 1992.
- Guiborg, S., P. Heinrich, and R. Roche, Numerical modeling of the 1995 Chilean tsunami, *Geophys. Res. Lett.*, 24(7), 775–778, 1997.
- Hasselmann, K., A statistical analysis of the generation of microseisms, *Rev. Geophys.*, 1, 177–209, 1963.
- Hasselmann, K. A., et al., Measurements of wind-driven growth and swell decay during the Joint North Sea Wave Project (JONSWAP), *Rep. 12*, 95 pp., Dtsch. Hydrogr. Inst., Hamburg, Germany, 1973.
- Haubrich, R. A., and K. McCamy, Microseisms: Coastal and pelagic sources, *Rev. Geophys.*, 7(3), 539–571, 1969.
- Haubrich, R. A., W. H. Munk, and F. E. Snodgrass, Comparative spectra of microseisms and swell, *Bull. Seismol. Soc. Am.*, 53, 27–37, 1963.
- Hedlin, M. A., and J. A. Orcutt, A comparative study of island, seafloor and subseafloor ambient noise levels, *Bull. Seismol. Soc. Am.*, 79(1), 172–179, 1989.
- Herbers, T. H. C., S. Elgar, and R. T. Guza, Infragravity-frequency (0.005–0.05 Hz) motions on the shelf, I, Forced waves, *J. Phys. Oceanogr.*, 24(5), 917–927, 1994.
- Herbers, T. H. C., S. Elgar, R. T. Guza, and W. C. O'Reilly, Infragravity-frequency (0.005–0.05 Hz) motions on the shelf, II, Free waves, *J. Phys. Oceanogr.*, 25(6), 1063–1079, 1995.
- Hermann, R. B., Focal depth determination from the signal character of long period  $p$  waves, *Bull. Seismol. Soc. Am.*, 66(4), 1221–1232, 1976.
- Houston, H., Broadband source spectrum, seismic energy and stress drop of the 1989 Macquarie ridge earthquake, *Geophys. Res. Lett.*, 17(7), 1021–1024, 1990.
- Houston, H., and H. Kanamori, Source spectra of great earthquakes: Teleseismic constraints on rupture process and strong motion, *Bull. Seismol. Soc. Am.*, 76(1), 19–42, 1986.
- Hunkins, A. K., Waves on the Arctic Ocean, *J. Geophys. Res.*, 67(6), 2477–2489, 1962.
- Huntley, D. A., R. T. Guza, and E. B. Thornton, Field observations of surf beat, 1, Progressive edge waves, *J. Geophys. Res.*, 86(C7), 6451–6466, 1981.
- Kanamori, H., and G. Stewart, Mode of the strain release along the Gibbs fracture zone, Mid-Atlantic Ridge, *Phys. Earth Planet. Inter.*, 11, 312–332, 1976.
- Kasahara, J., S. Nagumo, S. Koresawa, T. Daikuhara, and H. Miyata, Experimental results of vortex generation around ocean bottom seismographs due to bottom current, *Bull. Earthquake Res. Inst. Univ. Tokyo*, 56, 169–182, 1980.
- Kasahara, J., H. Utada, T. Sato, and H. Kinoshita, A submarine cable OBS by use of the retired telecommunication cable: GeoTOC program, paper presented at International Workshop on Scientific Use of Submarine Cables, Comm. for Sci. Use of Submarine Cables, Okinawa, Japan, Feb. 25–28, 1997.
- Kibblewhite, A. C., and K. C. Ewans, Wave-wave interactions, microseisms and infrasonic ambient noise in the ocean, *J. Acoust. Soc. Am.*, 78(3), 981–994, 1985.
- Kibblewhite, A. C., and C. Y. Wu, The theoretical description of wave-wave interactions as a source of noise in the ocean, *J. Acoust. Soc. Am.*, 89(5), 2241–2252, 1991.
- Kinsman, B., *Wind Waves: Their Generation and Propagation on the Ocean Surface*, 676 pp., Prentice-Hall, Englewood Cliffs, N. J., 1984.
- Lacoss, R. T., E. J. Kelly, and M. N. Toksoz, Estimation of seismic noise structure using arrays, *Geophysics*, 34(1), 21–38, 1969.
- Lahav, D., J. A. Orcutt, C. S. Cox, and P. M. Shearer, Low

- frequency sea floor noise from OBS hydrophone data (abstract), *Eos Trans. AGU*, 67(44), 1084, 1986.
- Levchenko, D. G., S. L. Soloviev, A. V. Son'kin, and E. V. Voronina, Recording of ocean-bottom seismic noise and of a strong earthquake in the Himalayas by broad band OBS installed on the Mid-Atlantic Ridge, *Phys. Earth Planet. Inter.*, 84, 305–320, 1994.
- Lewis, B. T. R., and J. McClain, Converted shear waves as seen by ocean bottom seismometers and surface buoys, *Bull. Seismol. Soc. Am.*, 67(5), 1291–1302, 1977.
- Lewis, B. T. R., and J. D. Tuthill, Instrumental waveform distortion on ocean bottom seismometers, *Mar. Geophys. Res.*, 5, 79–85, 1981.
- Li, Y., W. Prothero, C. Thurber, and R. Butler, Observations of ambient noise and coherency on the island of Hawaii for teleseismic studies, *Bull. Seismol. Soc. Am.*, 84(4), 1229–1242, 1994.
- Lighthill, J., *Waves in Fluids*, p. 504, Cambridge Univ. Press, New York, 1979.
- Liu, J.-Y., and H. Schmidt, Effect of rough seabed on the spectral composition of deep ocean infrasonic ambient noise, *J. Acoust. Soc. Am.*, 93(2), 753–769, 1993.
- Longuet-Higgins, M. S., A theory for the generation of microseisms, *Philos. Trans. R. Soc. London, Ser. A*, 243, 1–35, 1950.
- Longuet-Higgins, M. S., and R. W. Stewart, Radiation stress in water waves: A physical discussion, with applications, *Deep Sea Res.*, 11, 529–562, 1964.
- Lonsdale, P., Inflow of bottom water in the Panama Basin, *Deep Sea Res.*, 24, 1065–1101, 1977.
- Luther, D. S., A. D. Chave, J. H. Filloux, and P. F. Spain, Evidence for local and nonlocal barotropic responses to atmospheric forcing during BEMPEX, *Geophys. Res. Lett.*, 17(7), 949–952, 1990.
- McCreery, C. S., F. K. Duennebie, and G. H. Sutton, Correlation of deep ocean noise (0.4–20 Hz) with wind, and the Holu spectrum—a worldwide constant, *J. Acoust. Soc. Am.*, 93(5), 2639–2648, 1993.
- McDonald, M. A., J. A. Hildebrand, and S. C. Webb, Blue and fin whales observed on a seafloor array in the northeast Pacific, *J. Acoust. Soc. Am.*, 98(2), 712–721, 1995.
- McDonough, R. N., and A. D. Whalen, *Detection of Signals in Noise*, p. 495, Academic, San Diego, Calif., 1995.
- Melton, B. S., The sensitivity and dynamic range of inertial seismographs, *Rev. Geophys.*, 14(1), 93–116, 1976.
- Menke, W., and R. Chen, Numerical studies of the coda fall off rate of multiple scattered waves in randomly layered media, *Bull. Seismol. Soc. Am.*, 74(4), 1605–1621, 1984.
- Montagner, J.-P., et al., The French pilot experiment OFM-SISOBS: First scientific results on noise level and event detection, *Phys. Earth Planet. Inter.*, 84, 321–336, 1994.
- Moore, R. D., L. M. Dorman, C.-Y. Huang, and D. L. Berliner, An ocean bottom, microprocessor based seismometer, *Mar. Geophys. Res.*, 4, 451–477, 1981.
- Munk, W., F. Snodgrass, and F. Gilbert, Long waves on the continental shelf: An experiment to separate trapped and leaky modes, *J. Fluid Mech.*, 20(4), 529–554, 1964.
- Naval Weather Service Detachment, *U.S. Navy Marine Climatic Atlas of the World*, vol. 1–8, U.S. Government Printing Office, Washington, D. C., 1974–1979.
- Novelo-Casanova, D. A., and R. Butler, High frequency seismic coda and scattering in the northwest Pacific, *Bull. Seismol. Soc. Am.*, 76(2), 617–626, 1986.
- Okamoto, T., and T. Miyatake, Effects of near source seafloor topography on long period teleseismic *P* waveforms, *Geophys. Res. Lett.*, 16(11), 1309–1312, 1989.
- Okihoro, M., R. T. Guza, and R. J. Seymour, Bound infragravity waves, *J. Geophys. Res.*, 97(C7), 11,453–11,469, 1992.
- Oliver, J., A worldwide storm of microseisms with periods of about 27 s, *Bull. Seismol. Soc. Am.*, 52(3), 507–517, 1962.
- Oltman-Shay, J., and R. T. Guza, Infragravity wave edge wave observations on two California beaches, *J. Phys. Oceanogr.*, 17(5), 644–663, 1987.
- Orcutt, J. A., Structure of the Earth: Oceanic crust and uppermost mantle, *Rev. Geophys.*, 25(6), 1177–1196, 1987.
- Orcutt, J. A., OSN pilot experiment becomes a reality, *JOI/USSAC Newsl.* 9(2), 12–14, Joint Oceanogr. Inst., Washington, D. C., 1996.
- Orcutt, J. A., and T. H. Jordan, MSS and OBS Data from the Ngenide experiment in the southwest Pacific, in *The VELA Program*, edited by A. Kerr, pp. 758–770, Def. Adv. Res. Proj. Agency, Washington, D. C., 1986.
- Ou, G.-B., and R. B. Hermann, A statistical model for the ground motion produced by earthquakes at local and regional distances, *Bull. Seismol. Soc. Am.*, 80(6), 1397–1417, 1990.
- Peterson, J., Observations and modeling of seismic background noise, *U. S. Geol. Surv. Open File Rep.*, 93-322, 1993.
- Pierson, W. J., and L. Moskowitz, A proposed spectral form for fully developed wind seas based on the similarity theory of S. A. Kitaigorodskii, *J. Geophys. Res.*, 69, 5181–5190, 1964.
- Purdy, G. M., and A. D. Dziewonski, *Proceedings of a Workshop on Broad Band Seismometers in the Deep Ocean*, 331 pp., Woods Hole Oceanogr. Inst., Woods Hole, Mass., 1988.
- Richards, P., and W. Menke, The apparent attenuation of a scattering medium, *Bull. Seismol. Soc. Am.*, 73(3), 1005–1021, 1983.
- Richardson, W. J., C. R. Greene, C. I. Malme, and D. H. Thomson, *Marine Mammals and Noise*, 576 pp., Academic, San Diego, Calif., 1995.
- Riedesel, M., J. A. Orcutt, K. C. McDonald, and J. S. McClain, Microearthquakes in the black smoker hydrothermal field, East Pacific Rise at 21°N, *J. Geophys. Res.*, 87(B13), 10,613–10,623, 1982.
- Riedesel, M. A., R. D. Moore, and J. A. Orcutt, Limits of sensitivity of inertial seismometers with velocity transducers and electronic amplifiers, *Bull. Seismol. Soc. Am.*, 80(6), 1725–1752, 1990.
- Rhines, P. B., The dynamics of unsteady currents, in *The Sea*, vol. 6, *Marine Modeling*, edited by E. D. Goldberg, et al., pp. 189–318, John Wiley, New York, 1977.
- Romanowicz, B., Seismic tomography of the Earth's mantle, *Annu. Rev. Earth Planet. Sci.*, 19, 77–99, 1991.
- Romanowicz, B., M. Cara, J.-F. Fels, and D. Rouland, GEO-SCOPE: A French initiative in long period three component global seismic networks, *Eos Trans. AGU*, 65(42), 1–4, 1984.
- Rowlett, H., and D. Forsyth, Teleseismic *P*-wave delay times in a major oceanic fracture zone, *Geophys. Res. Lett.*, 6(4), 273–276, 1979.
- Sandwell, D. T., and R. W. Agreen, Seasonal variation in wind speed and sea state from global satellite measurements, *J. Geophys. Res.*, 89(C2), 2041–2051, 1984.
- Sato, T., K. Katsumata, J. Kasahara, N. Hirata, R. Hino, N. Takahashi, M. Sekine, S. Miura, and S. Koresawa, Travel time residuals of teleseismic *P*-waves at the Rodriguez triple junction in the Indian Ocean using ocean bottom seismometers, *Geophys. Res. Lett.*, 23(7), 713–716, 1996.
- Sauter, A. W., Studies of the upper oceanic crust using ocean bottom seismometers, Ph.D. thesis, 100 pp., Univ. of Calif., San Diego, La Jolla, 1987.
- Sauter, A., J. Hallinan, R. Carrier, B. Wooding, A. Schultz, and L. Dorman, A new ocean bottom seismometer, in *Proceedings of Conference: Marine Instrumentation*, '90, pp. 99–104, Mar. Technol. Soc., Washington, D. C., 1990.
- Schmidt, H., and W. A. Kuperman, Estimation of surface noise

- source level from low-frequency seismoacoustic ambient noise measurements, *J. Acoust. Soc. Am.*, 84(6), 2153–2162, 1989.
- Scholz, C. H., *The Mechanics of Earthquakes and Faulting*, 439 pp., Cambridge Univ. Press, New York, 1990.
- Schreiner, A. E., and L. M. Dorman, Coherence lengths of seafloor noise: Effect of ocean bottom structure, *J. Acoust. Soc. Am.*, 88(3), 1503–1514, 1990.
- Scofield, J. H., J. V. Mantese, and W. W. Webb,  $1/f$  noise of metals: A case for intrinsic origin, *Phys. Rev. B*, 32(2), 736–742, 1985.
- Sereno, T., and J. Orcutt, Synthesis of realistic oceanic  $Pn$  wave trains, *J. Geophys. Res.*, 90(B14), 12,755–12,776, 1985.
- Sereno, T. J., and J. A. Orcutt, Synthetic  $Pn$  and  $Sn$  phases and the frequency dependence of  $Q$  of the oceanic lithosphere, *J. Geophys. Res.*, 92(B5), 3541–3566, 1987.
- Silver, P. G., S. L. Beck, T. C. Wallace, C. Meade, S. C. Myers, D. E. James, and R. Kuehnel, Rupture characteristics of the deep Bolivian earthquake of 9 June 1994 and the mechanism of deep focus earthquakes, *Science*, 268, 69–73, 1995.
- Snodgrass, F. E., G. W. Groves, K. F. Hasselmann, G. R. Miller, W. H. Munk, and W. H. Powers, Propagation of ocean swell across the Pacific, *Philos. Trans. R. Soc. London, Ser. A*, 259(1103), 431–497, 1966.
- Sohn, R. A., J. A. Hildebrand, S. C. Webb, and C. G. Fox, Hydrothermal microseismicity at the megaplume site on the southern Juan de Fuca ridge, *Bull. Seismol. Soc. Am.*, 85(3), 775–786, 1995.
- Sorrells, G. G., A preliminary investigation into the relationship between long-period seismic noise and local fluctuations in the atmospheric pressure field, *Geophys. J. R. Astron. Soc.*, 226, 71–82, 1971.
- Sorrells, G. G., and E. J. Douze, A preliminary report on infrasonic waves as a source of long-period seismic noise, *J. Geophys. Res.*, 79, 4908–4917, 1974.
- Sorrells, G. G., and T. T. Goforth, Low frequency Earth motion generated by slowly propagating partially organized pressure fields, *Bull. Seismol. Soc. Am.*, 63, 1583–1601, 1973.
- Stein, S., and D. A. Wiens, Depth determination for shallow teleseismic earthquakes: Methods and results, *Rev. Geophys.*, 24(4), 806–832, 1986.
- Stephen, R. A., and S. A. Swift, Modeling seafloor geoaoustic interaction with a numerical scattering chamber, *J. Acoust. Soc. Am.*, 96(2), 973–990, 1994.
- Stephen, R. A., et al., The seafloor borehole seismic system (SEABASS) and ULF noise, *Mar. Geophys. Res.*, 16, 243–269, 1994.
- Sutton, G. H., and N. Barstow, Ocean bottom ultra low frequency (ULF) seismo-acoustic ambient noise: 0.002–0.4 Hz, *J. Acoust. Soc. Am.*, 87, 2005–2012, 1990.
- Sutton, G. H., W. G. McDonnell, D. D. Prentiss, and S. N. Thanos, Ocean bottom seismic observatories, *Proc. IEEE*, 53, 1909–1921, 1965.
- Sutton, G. H., F. K. Duennebie, and B. Iwatake, Coupling of ocean bottom seismometers to soft bottom, *Mar. Geophys. Res.*, 5, 35–51, 1981.
- Suyehiro, K., T. Kanazawa, N. Hirata, and M. Shinohara, Ocean downhole seismic project, *J. Phys. Earth*, 43, 599–618, 1995.
- Symonds, G., D. A. Huntley, and A. J. Bowen, Two-dimensional surf beat: Long wave generation by a time varying break point, *J. Geophys. Res.*, 87, 492–498, 1982.
- Trehu, A. M., Lateral velocity variations in the Orozco transform fault inferred from observed incident angles and azimuths of  $P$ -waves, *Geophys. J. R. Astron. Soc.*, 177, 711–728, 1984.
- Trehu, A. M., Coupling of ocean bottom seismometers to sediment: Results from tests with the USGS ocean bottom seismometer, *Bull. Seismol. Soc. Am.*, 75(1), 271–289, 1985a.
- Trehu, A. M., A note on the effect of bottom currents on an ocean bottom seismometer, *Bull. Seismol. Soc. Am.*, 75(4), 1195–1204, 1985b.
- Trehu, A. M., and S. C. Solomon, Coupling parameters of the MIT OBS at two nearshore sites, *Mar. Geophys. Res.*, 5, 68–78, 1981.
- Trehu, A. M., and G. H. Sutton, A note on the seafloor coupling characteristics of the new ONR ocean bottom seismometer, *Mar. Geophys. Res.*, 16, 91–103, 1994.
- Trevorrow, M., T. Yamamoto, A. Turgut, D. Goodman, and M. Badiy, Very low frequency ocean bottom noise and coupling on the shallow continental shelf, *Mar. Geophys. Res.*, 11, 129–152, 1989.
- Urick, R. J., *Principles of Underwater Sound*, 3rd ed., 423 pp., McGraw-Hill, New York, 1983.
- VanDorn, W. G., Some tsunami characteristics deducible from tide records, *J. Phys. Oceanogr.*, 14(2), 353–363, 1984.
- VanDorn, W. G., Tide gauge response to tsunamis, II, Other oceans and smaller seas, *J. Phys. Oceanogr.*, 17(9), 1507–1516, 1987.
- Walker, D., High frequency  $Pn$  and  $Sn$  phases: Some comparisons for the western central and south Pacific, *Geophys. Res. Lett.*, 8, 207–209, 1981.
- Walker, D., Deep ocean seismology, *Eos Trans. AGU*, 65(1), 2–4, 1984.
- Walker, D., and C. S. McCreery, Significant unreported earthquakes in “aseismic” regions of the western Pacific, *Geophys. Res. Lett.*, 12, 433–436, 1985.
- Walker, D. A., C. S. McCreery, and G. H. Sutton, Spectral characteristics of high-frequency  $Pn$ ,  $Sn$  phases in the western Pacific, *J. Geophys. Res.*, 88(B5), 4289–4298, 1983.
- Ward, S. N., Ringing  $P$  waves and submarine faulting, *J. Geophys. Res.*, 84(B6), 3057–3062, 1979.
- Webb, S. C., Long period acoustic and seismic measurements and ocean floor currents, *IEEE J. Oceanic Eng.*, 13, 263–270, 1988.
- Webb, S. C., The equilibrium microseism spectrum, *J. Acoust. Soc. Am.*, 92(4), 2141–2158, 1992.
- Webb, S. C., and C. S. Cox, Observations and modeling of seafloor microseisms, *J. Geophys. Res.*, 91, 7343–7358, 1986.
- Webb, S. C., and A. D. Schultz, Very low frequency ambient noise at the seafloor under the Beafort Sea icecap, *J. Acoust. Soc. Am.*, 91(3), 1429–1439, 1992.
- Webb, S. C., X. Zhang, and W. C. Crawford, Infragravity waves in the deep ocean, *J. Geophys. Res.*, 96(C2), 2723–2736, 1991.
- Webb, S. C., W. C. Crawford, and J. A. Hildebrand, Long period seismometer deployed at OSN-1, *Seismic Waves*, 3(1), 4–6, 1994.
- Wenz, G. M., Acoustic ambient noise in the ocean: Spectra and sources, *J. Acoust. Soc. Am.*, 34(12), 1936–1956, 1962.
- Wiens, D. A., Bathymetric effects on body waveforms from shallow subduction zone earthquakes and application to seismic processes in the Kurile trench, *J. Geophys. Res.*, 94(B3), 2955–2972, 1989.
- Wyssession, M. E., How well do we utilize global seismicity?, *Bull. Seismol. Soc. Am.*, 86(5), 1207–1219, 1996.
- Yamamoto, T., and T. Torii, Seabed shear modulus profile inversion using surface gravity (water) wave-induced bottom motion, *Geophys. J. R. Astron. Soc.*, 85, 413–431, 1986.
- Yamamoto, T., M. V. Trevorrow, M. Badiy, and A. Turgut, Determination of the seabed porosity and shear modulus profiles using a gravity wave inversion, *Geophys. J. Int.*, 98, 173–182, 1989.
- Zakarauskas, P., Ambient noise in the sea: A literature review, *Can. Acoust.*, 14(3), 3–17, 1986.
- Zelikovitz, S. J., and W. A. Prothero Jr., The vertical response of

- an ocean bottom seismometer: Analysis of the Lopez Island vertical transient tests, *Mar. Geophys. Res.*, 5, 53–57, 1981.
- Zhang, J., and C. A. Langston, Constraints on oceanic lithosphere from deep focus regional earthquake receiver function inversions, *J. Geophys. Res.*, 100(B11), 22,187–22,196, 1995.
- Zhao, D., D. A. Wiens, L. Dorman, J. Hildebrand, S. Webb, and M. McDonald, High-resolution seismic tomography of the Tonga slab and Lau back arc basin (abstract), *Eos Trans. AGU*, 76(46), Fall Meet. Suppl., F392, 1995.
- Zurn, W., and R. Widmer, On noise reduction in vertical seismic records below 2 mHz using local barometric pressure, *Geophys. Res. Lett.*, 22(24), 3537–3540, 1995.

---

S. C. Webb, Marine Physics Laboratory, 0205, Scripps Institution of Oceanography, University of California, San Diego, 9500 Gilman Drive, La Jolla, CA 92093-0205. (e-mail: swebb@ucsd.edu)